



Probing continua of excitations in Kitaev spin liquids

Natalia Perkins

University of Minnesota

KITP, Intertwined17



Ceci n'est pas un chapeau.



Collaborators



Gábor Halász
(KITP,UCSB)



Johannes Knolle
Cambridge UK



Jeroen van den Brink
(IFW, Dresden)



Dima Kovrizhin
Cambridge UK



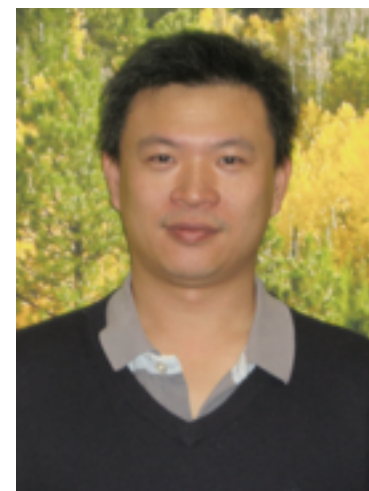
Brent Perreault
(UMN)



Roderich Moessner
MPIPKS, Dresden



Fiona Burnell
(UMN)

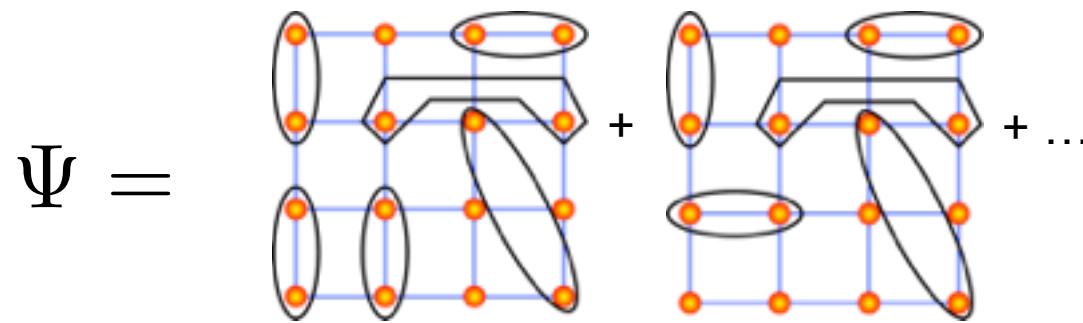


Gia-Wei Chern
University of Virginia

Quantum spin liquids

QSL: State of interacting spins that breaks no rotational or translational symmetry and has only short range spin correlations.

1973: Anderson proposes the “Resonating Valence Bond” state - a prototype of the modern QSLs

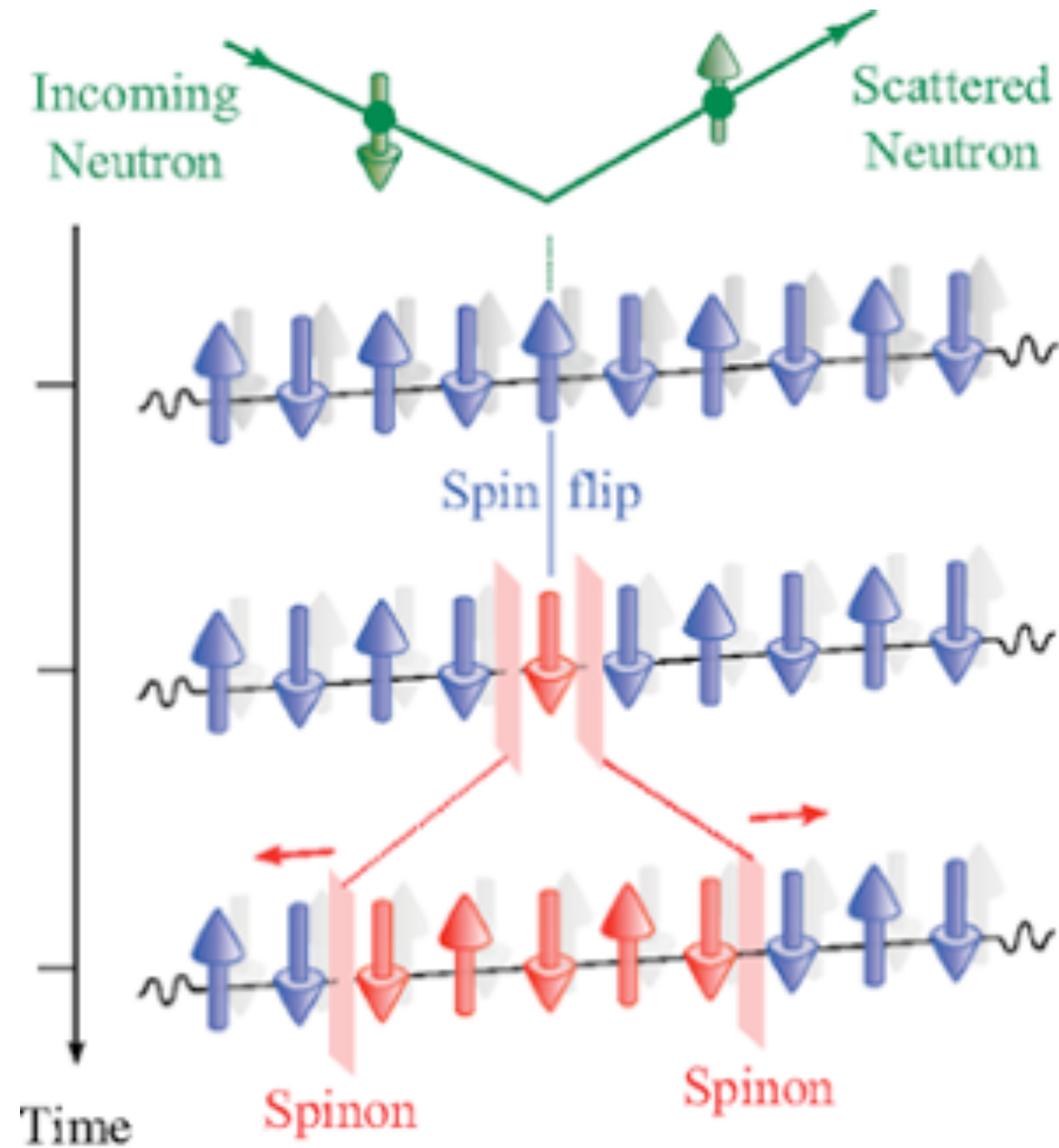


Unlike states with broken symmetry, QSLs are not characterized by any local order parameter.

QSLs are characterized by topological order and long range entanglement (difficult to probe experimentally).

QSLs supports excitations with *fractional quantum numbers and statistics*.

Example: Fractionalized excitations in spin-1/2 Heisenberg AFM chain



Many different quantum spin liquids

- Topological gapped QSLs

Quantum dimer model, toric code model...

- Spinon Fermi surface QSLs

Triangular lattice quantum spin liquid (YbMgGaO₄)

- Variety of Kitaev gapless QSLs with nodal Majorana fermion band structures

Hyperhoneycomb with nodal lines of Dirac cones,
hyperoctagon with Majorana fermions Fermi surface..

- U(1) QSL with gapless emergent photon

Quantum spin ice

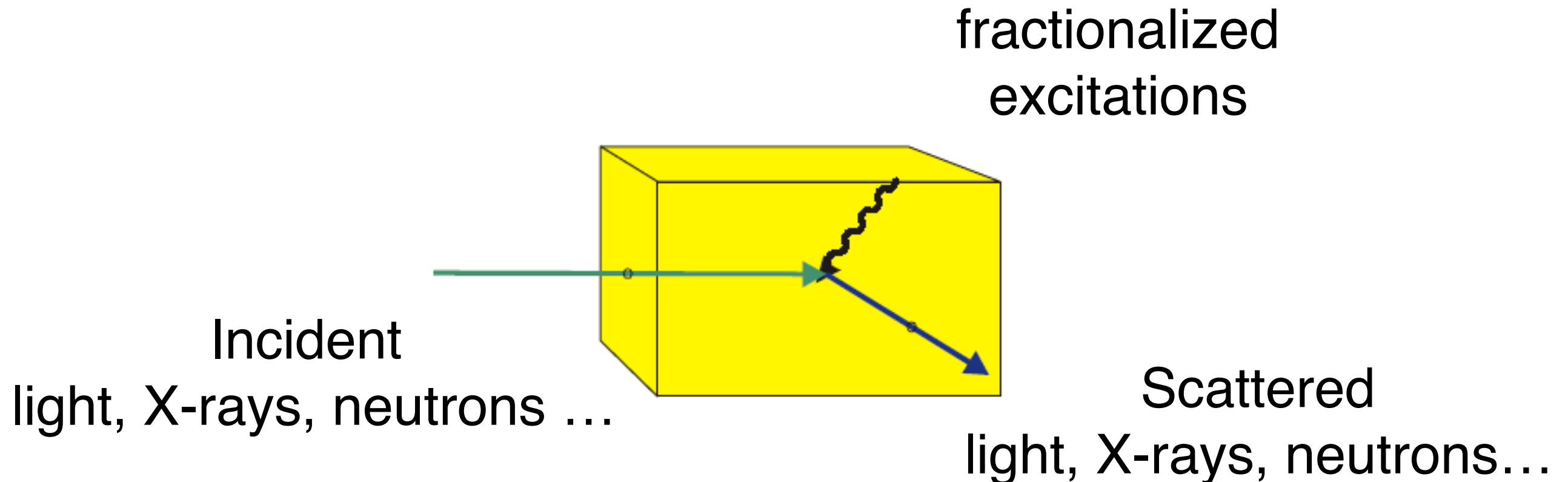
Quantum spin liquids

Main Question:

How to probe QSLs and their statistics?

Take home message:

Signatures of quantum order are mainly in the excitations

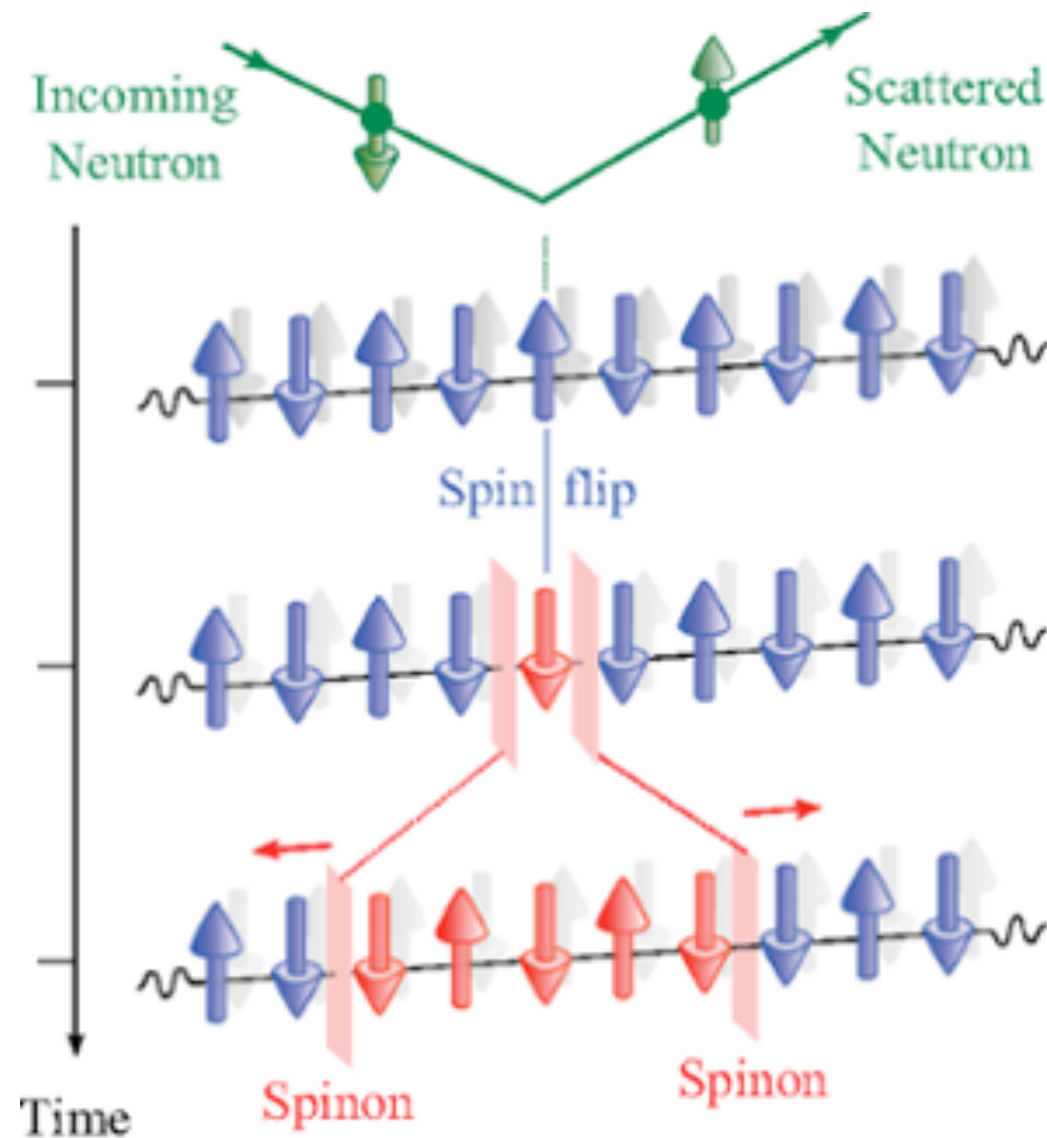


Response from QSL is always a multi-particle continuum

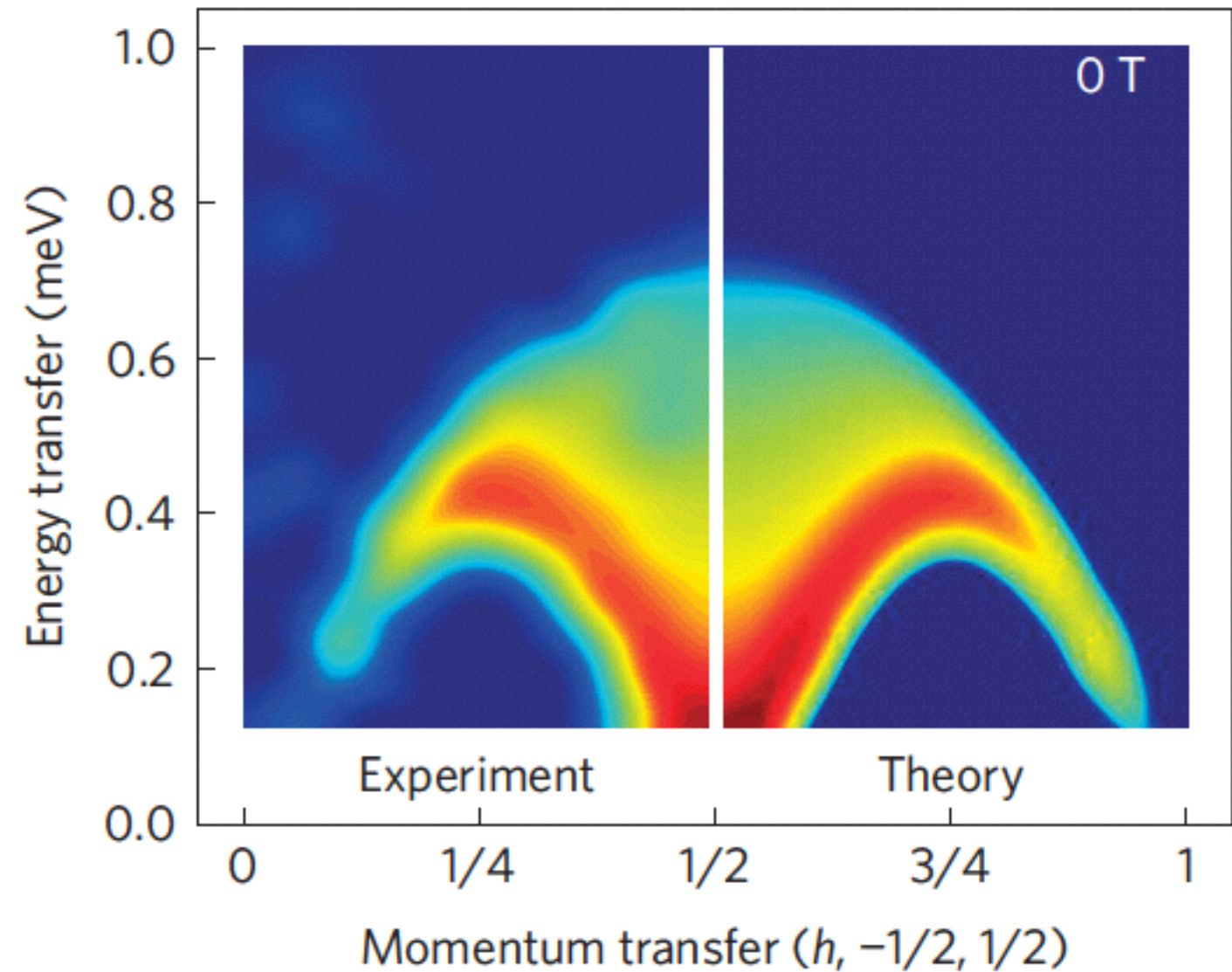
Since excitations carry fractional quantum numbers relative to the local degrees of freedom, only multiple quasiparticles can couple to external probes.



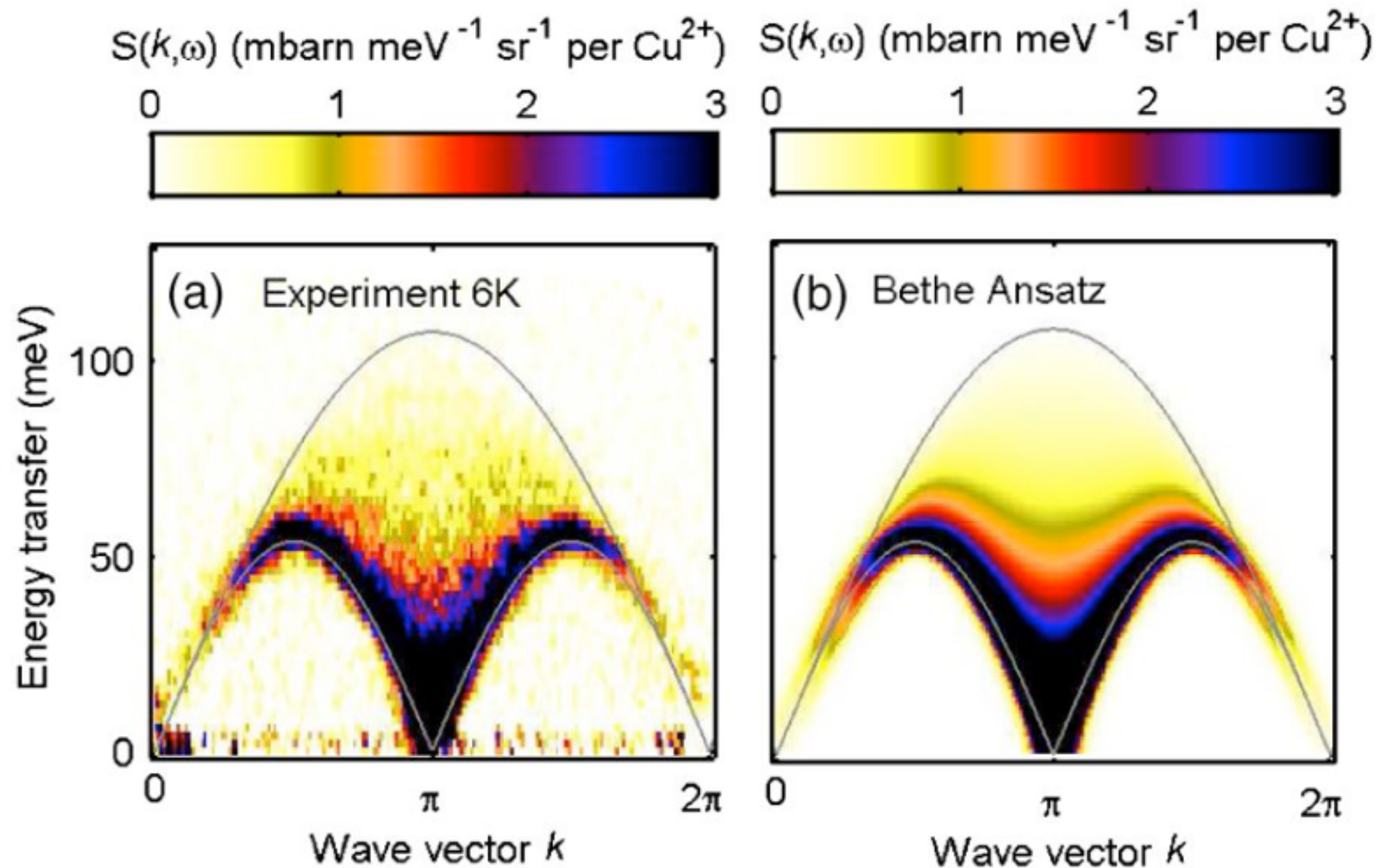
Spinon excitations in spin-1/2 Heisenberg AFM chain



d



Spinon excitations probed by neutrons: KCuF_3



The fractionalization was definitively identified by excellent **quantitative** agreement between experiments and exact calculation based on the Bethe Ansatz.

Poor understanding of strongly interacting systems beyond 1D

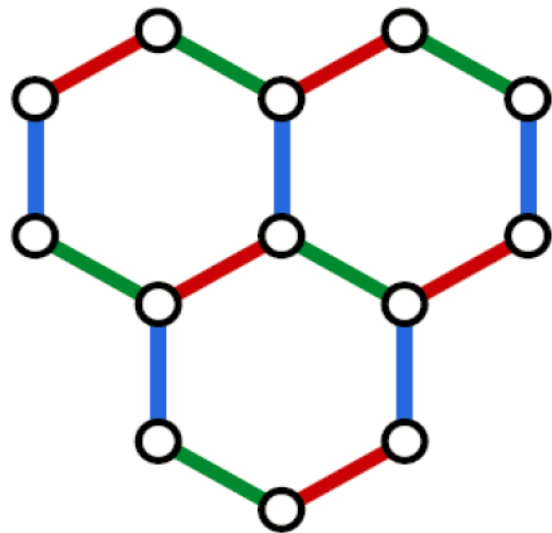
No exact results, only numerics or uncontrolled approximations

Kitaev Spin Liquids



Kitaev model on the honeycomb lattice

$$H = - \sum_{x\text{-bonds}} J_x \sigma_j^x \sigma_k^x - \sum_{y\text{-bonds}} J_y \sigma_j^y \sigma_k^y - \sum_{z\text{-bonds}} J_z \sigma_j^z \sigma_k^z$$



$$\begin{aligned} \sigma^x \sigma^x & \text{ (red bond)} \\ \sigma^y \sigma^y & \text{ (green bond)} \\ \sigma^z \sigma^z & \text{ (blue bond)} \end{aligned}$$

Exactly solvable 2D model

Spin liquid ground state

Fractionalized excitation

Mapping spins to Majorana fermions:

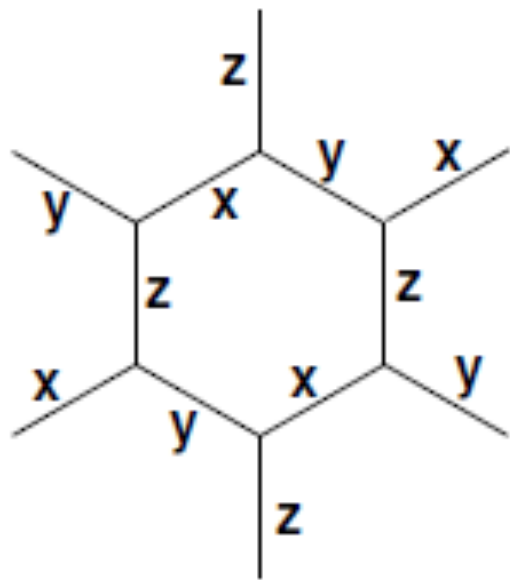
$$\sigma_i^a = i c_i c_i^a, \quad a = x, y, z$$

Spin fractionalization and Majorana fermions

Large number of conserved quantities,
local plaquette operators:

$$\tilde{W}_p = \hat{\sigma}_1^x \hat{\sigma}_2^y \hat{\sigma}_3^z \hat{\sigma}_4^x \hat{\sigma}_5^y \hat{\sigma}_6^z$$

$$[\tilde{W}_p, \hat{H}] = 0 \quad [\tilde{W}_p, \tilde{W}'_p] = 0$$



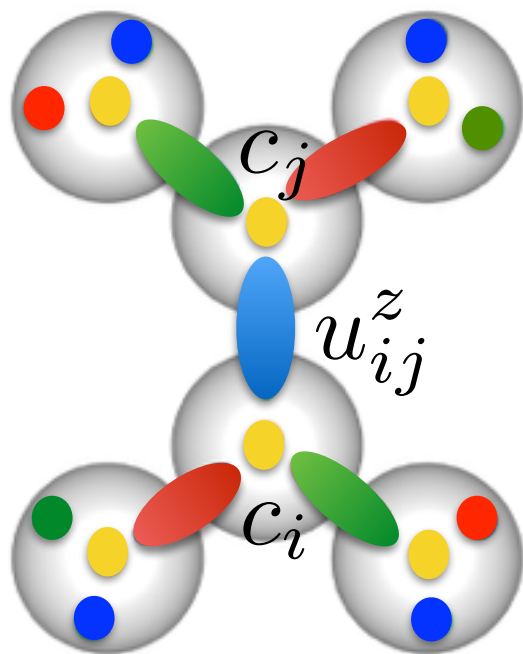
The Hilbert space can be separated into sectors
corresponding to eigenvalues

$$W_p = \pm 1$$

Quadratic Hamiltonian in each flux sector:

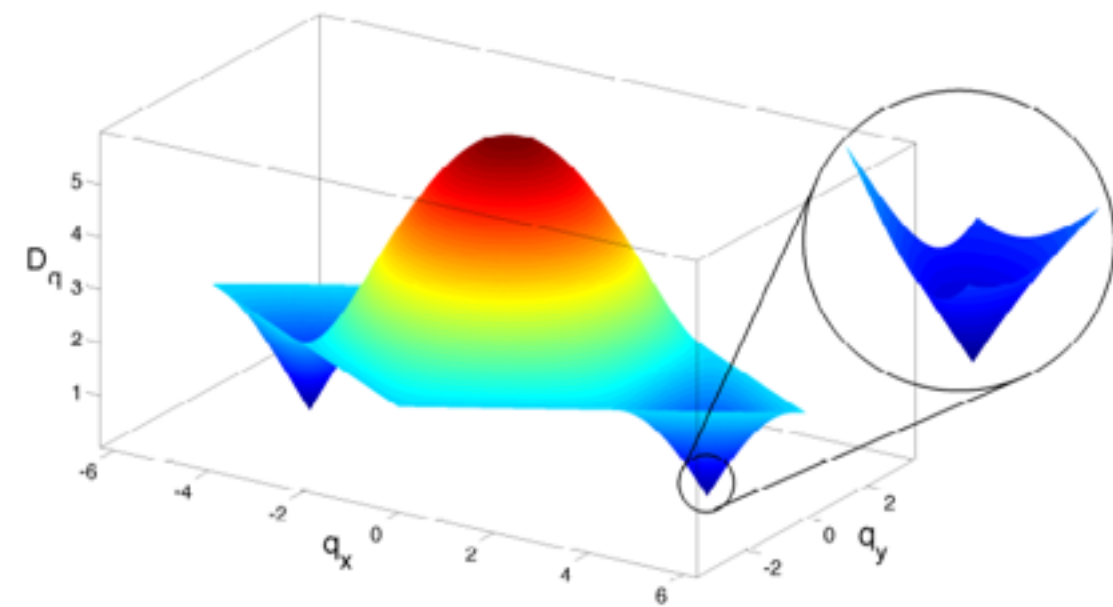
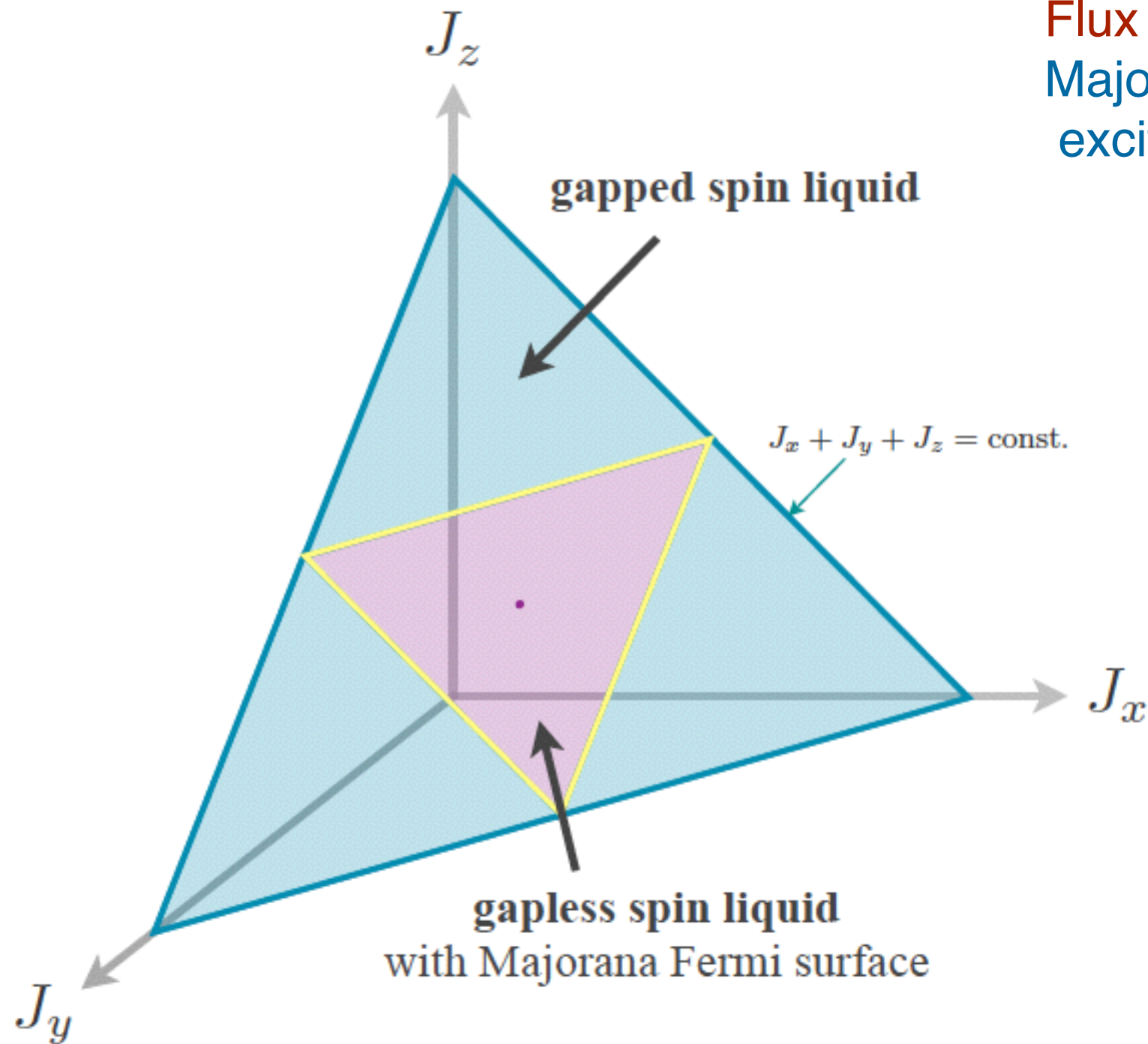
$$H = - \sum_{a=x,y,z} J_a \sum_{\langle ij \rangle_a} i c_i \hat{u}_{\langle ij \rangle_a} c_j$$

$$\hat{u}_{\langle ij \rangle_a} \equiv i c_i^a c_j^a$$



Excitations in the 2D Kitaev spin liquid

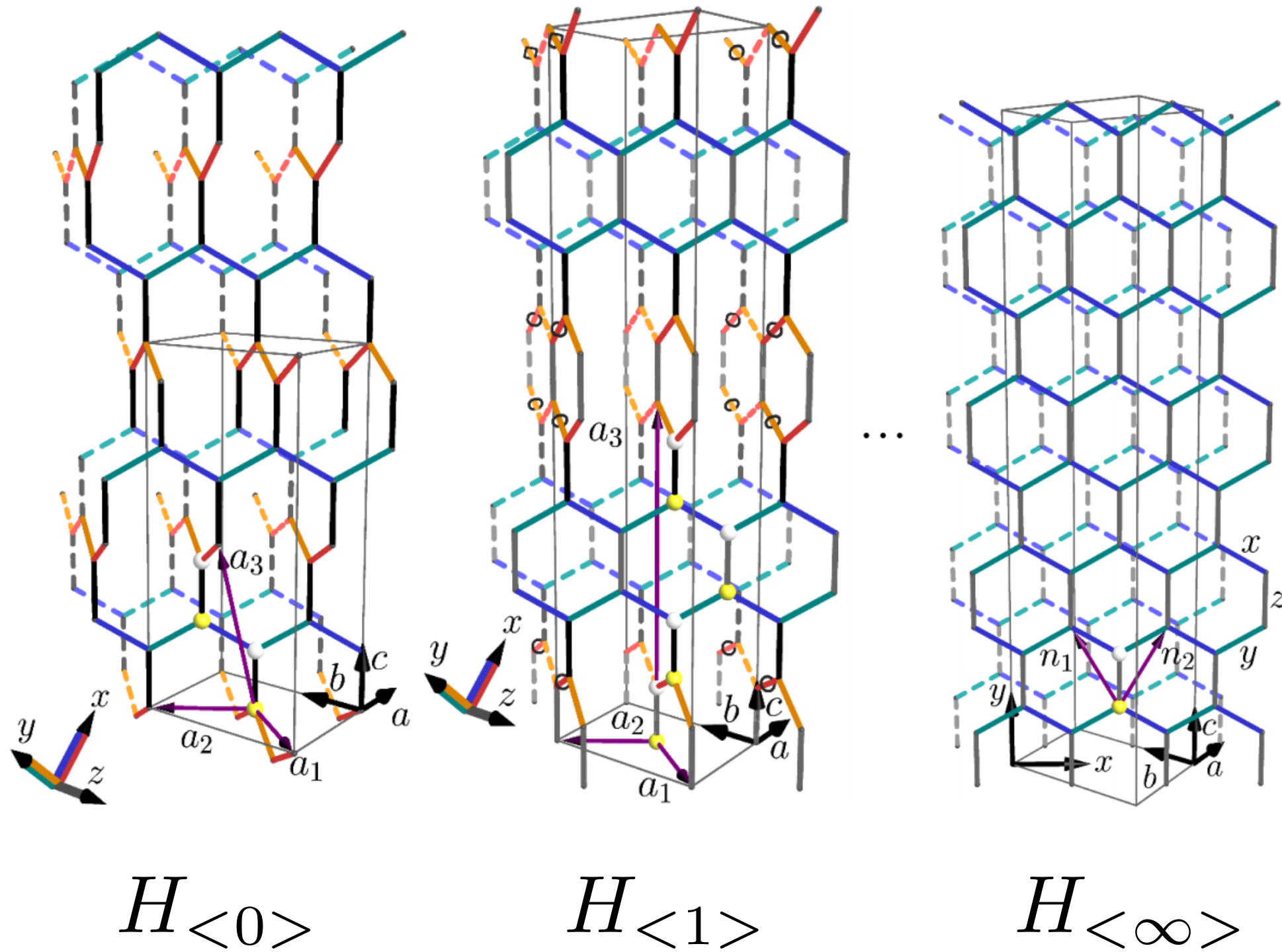
Flux excitations are always gapped.
Majorana fermion (spinon)
excitations are gapped or gapless.



Majorana fermion excitation spectrum
in the gapless phase

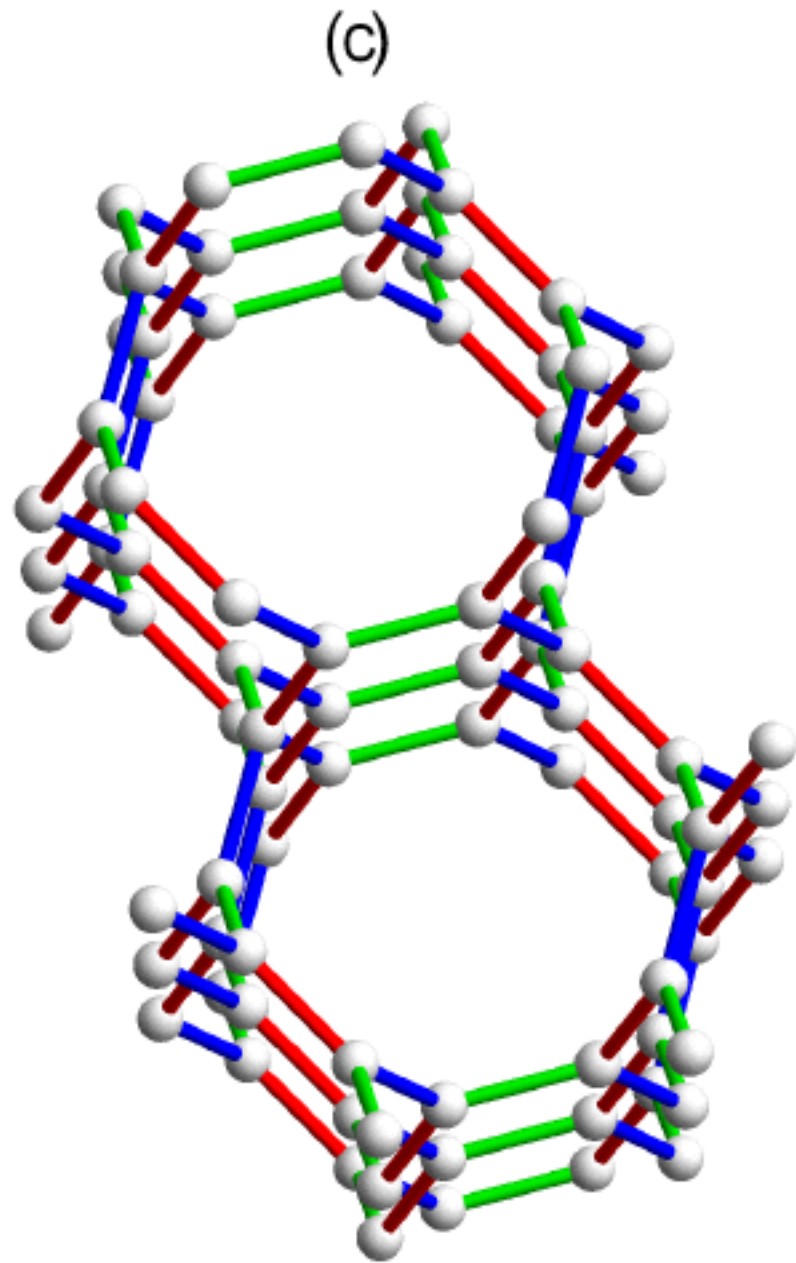
Fig. from M. Hermanns et al, 2014

3D Kitaev family

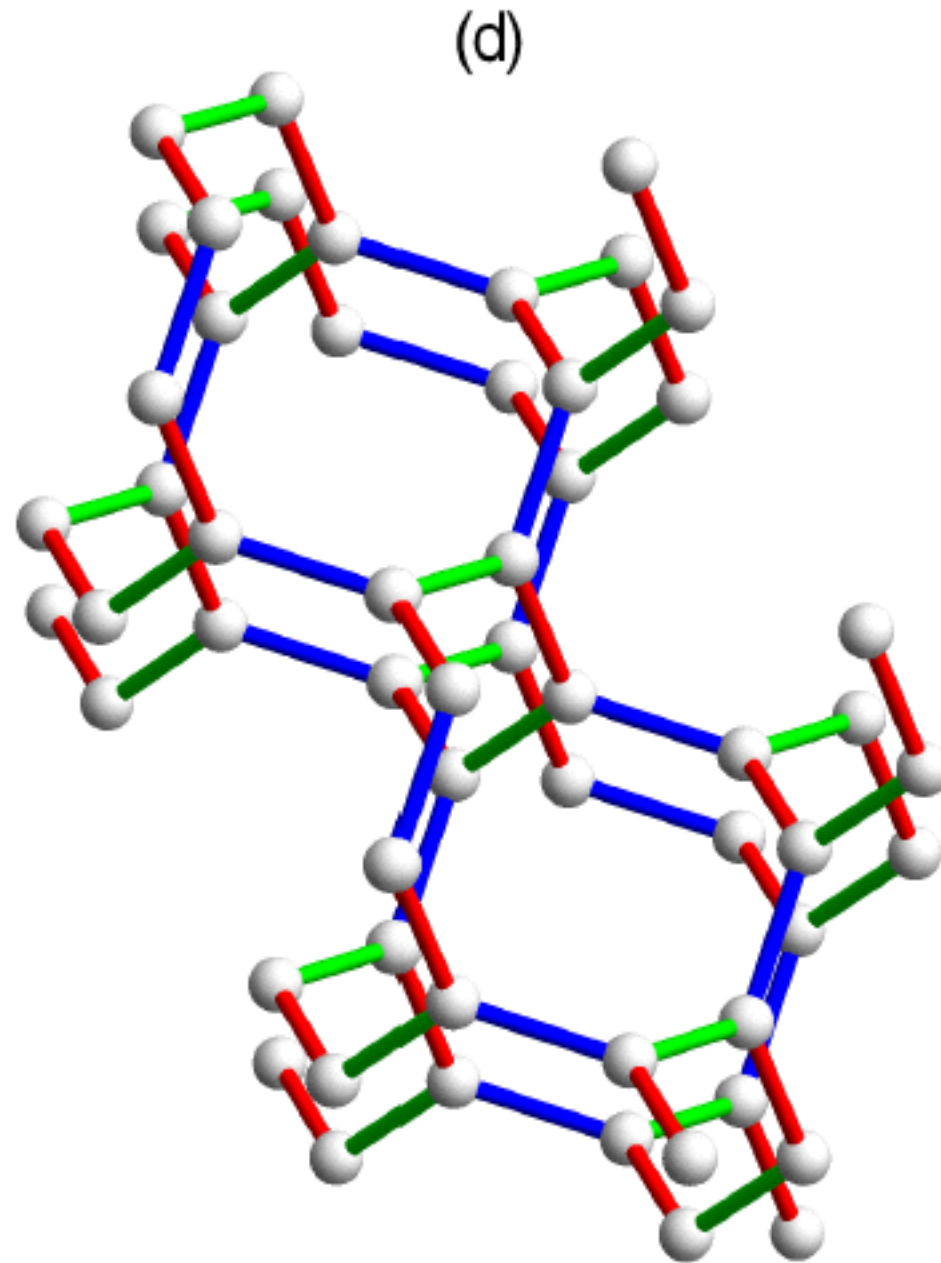


Hyperhoneycomb lattices

3D Kitaev family



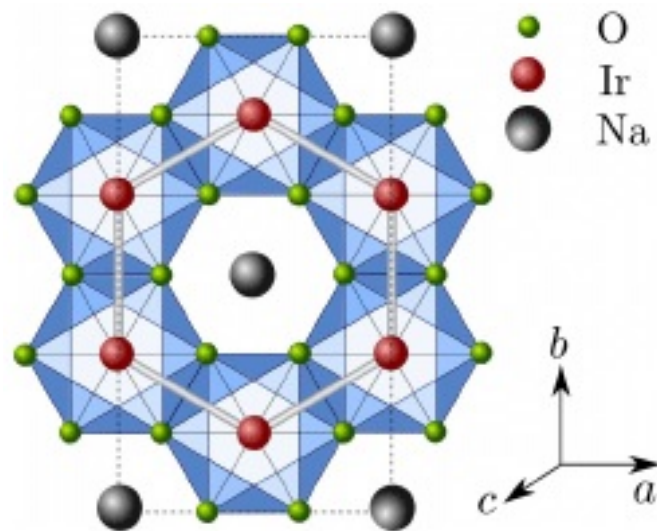
Hyperhexagon



Hypercuboctagon

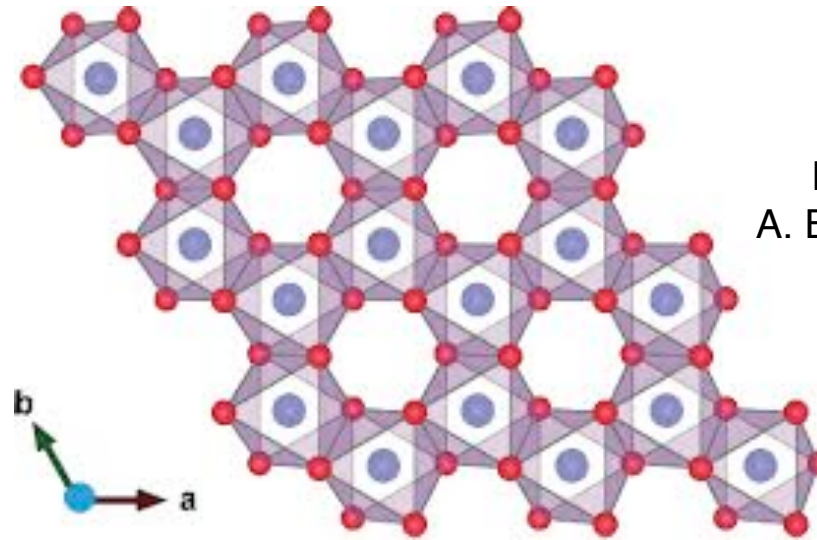
Experimental realizations

Na_2IrO_3
 $\alpha\text{-Li}_2\text{IrO}_3$



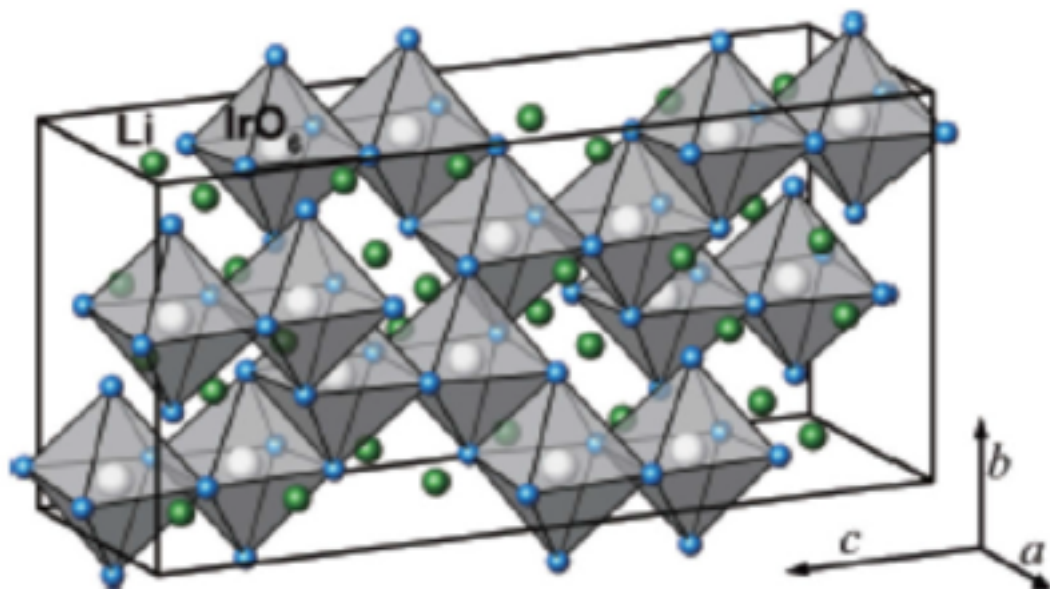
Y.Singh, P. Gegenwart,
PRL 2010, 2011

$\alpha\text{-RuCl}_3$



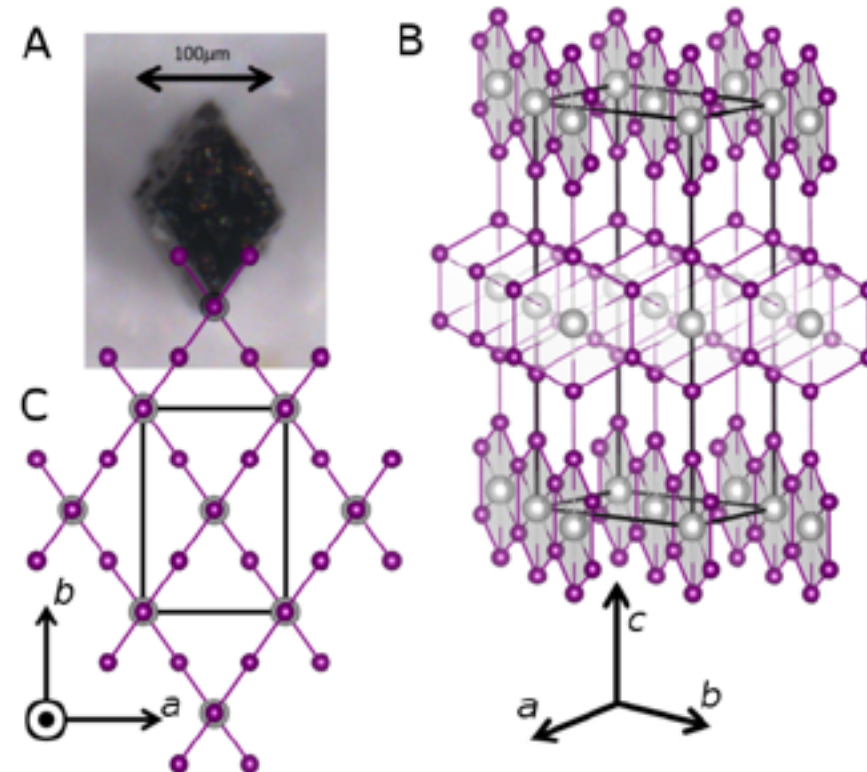
K. Plumb et al, Phys. Rev. B (2014)
A. Banerjee et al, Nature Materials (2016)

$\beta\text{-Li}_2\text{IrO}_3$



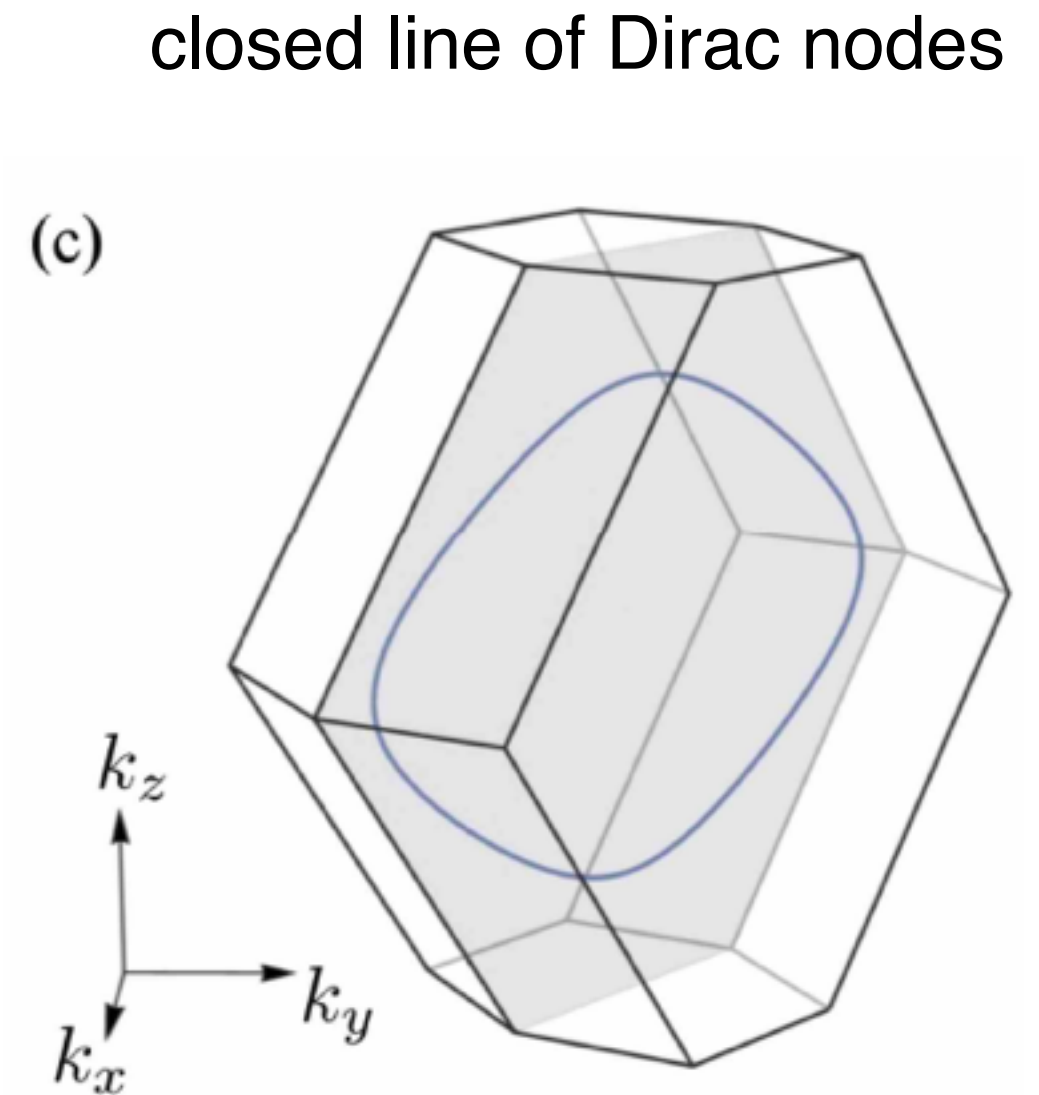
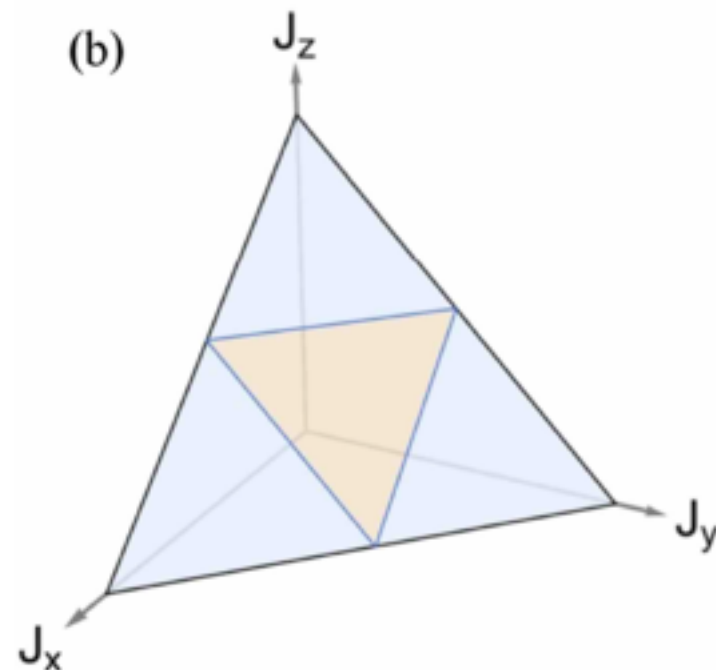
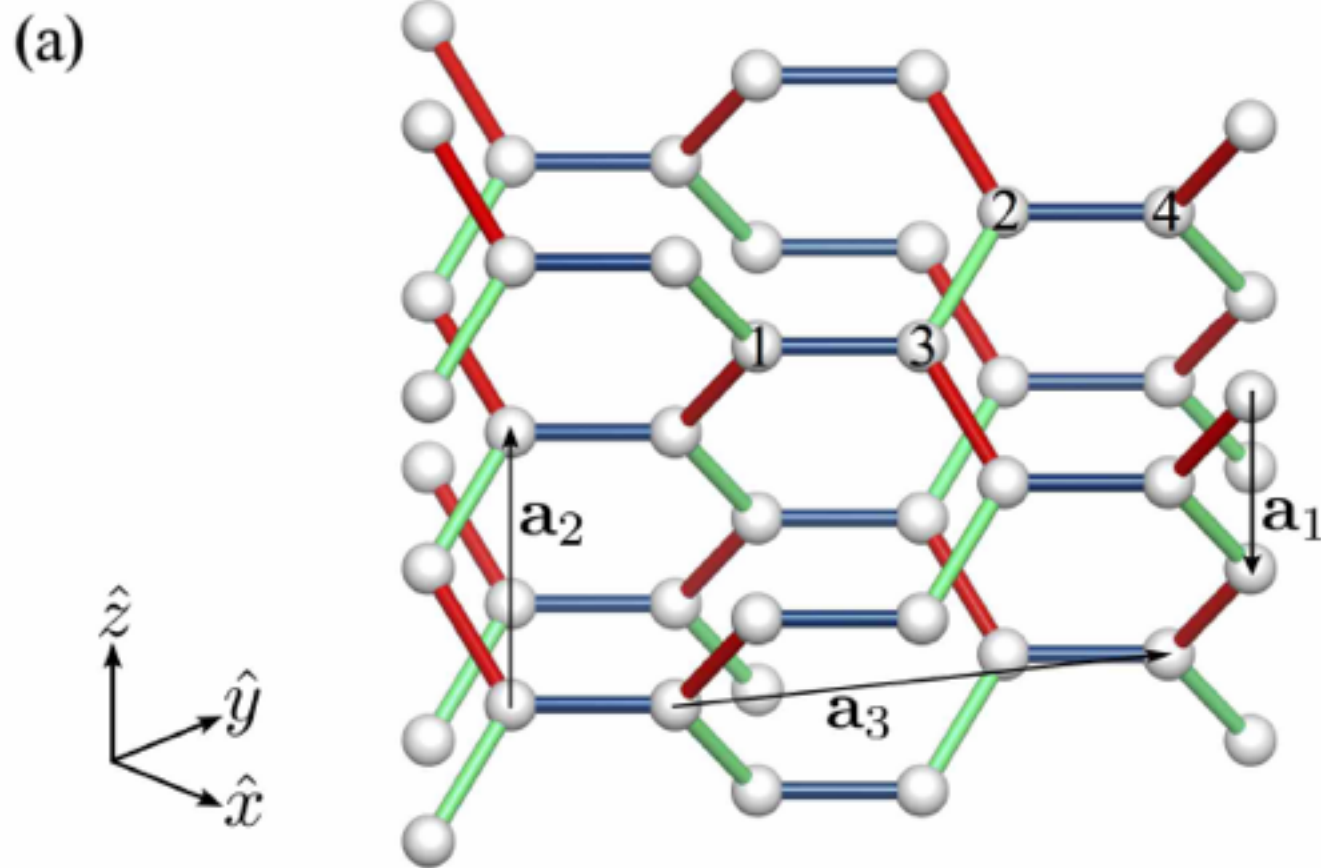
T. Takayama et al, PRL (2015)

$\gamma\text{-Li}_2\text{IrO}_3$



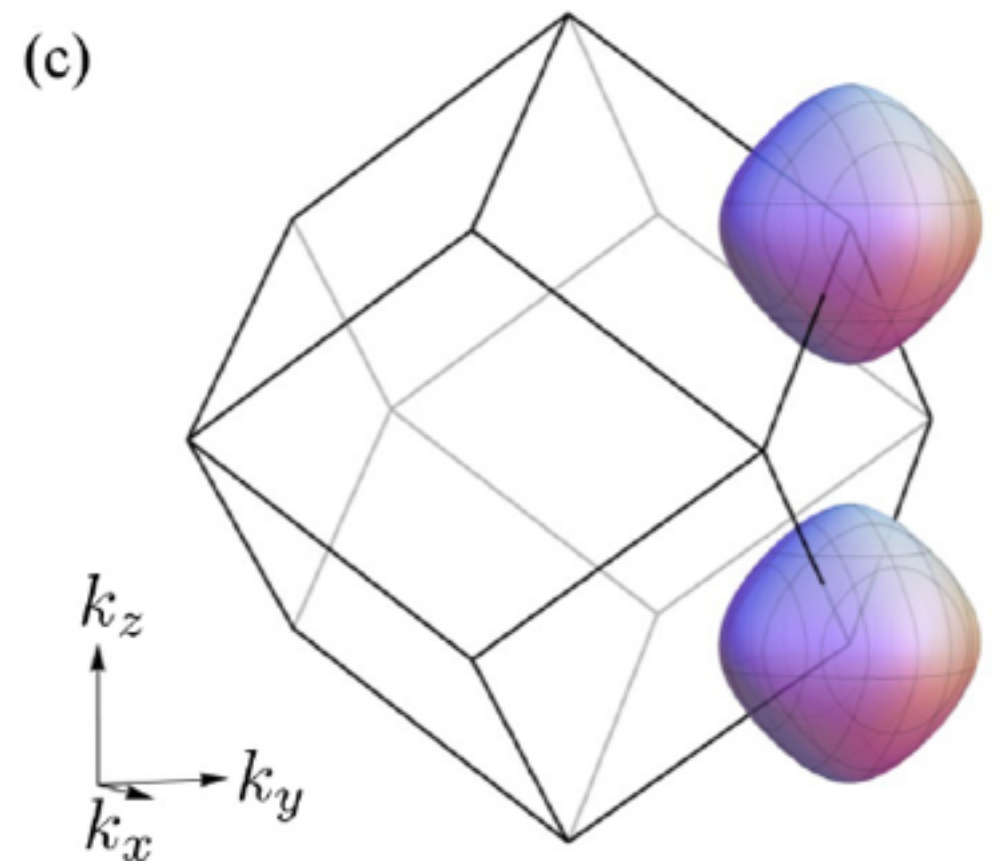
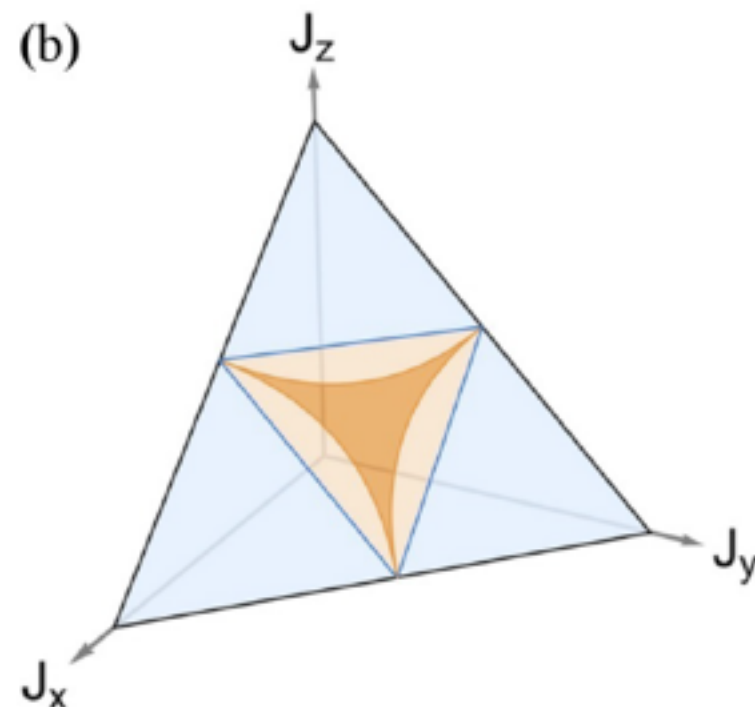
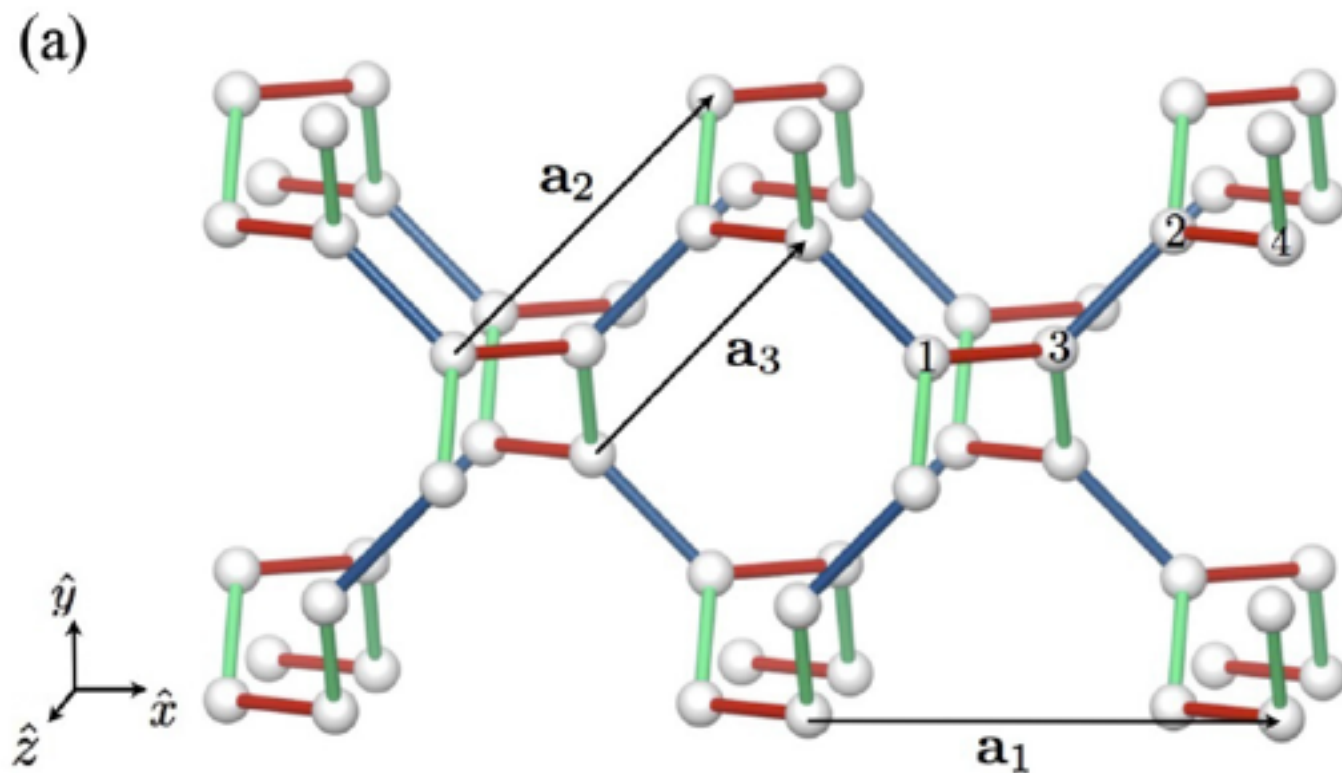
Modic, Nature Communications 5, 4203 (2014)

Hyperhoneycomb lattice

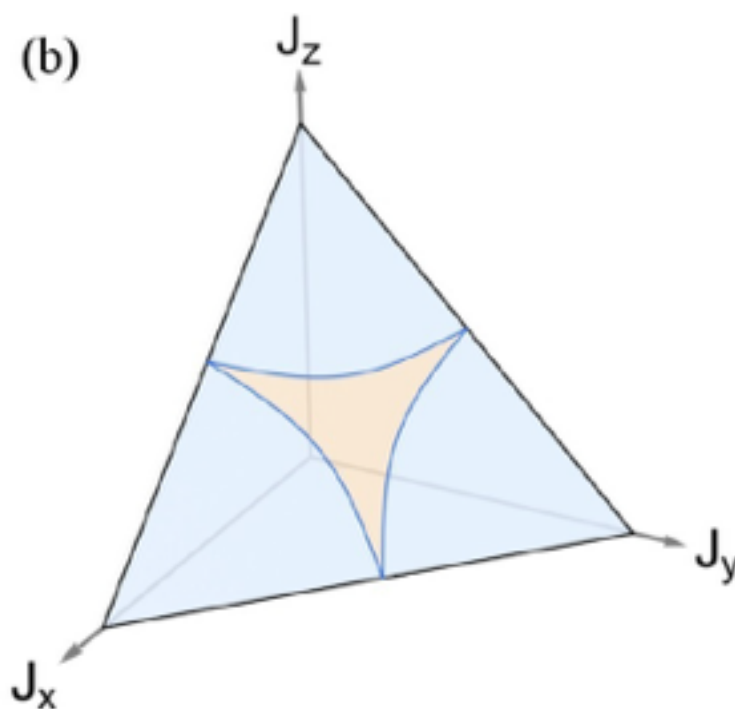
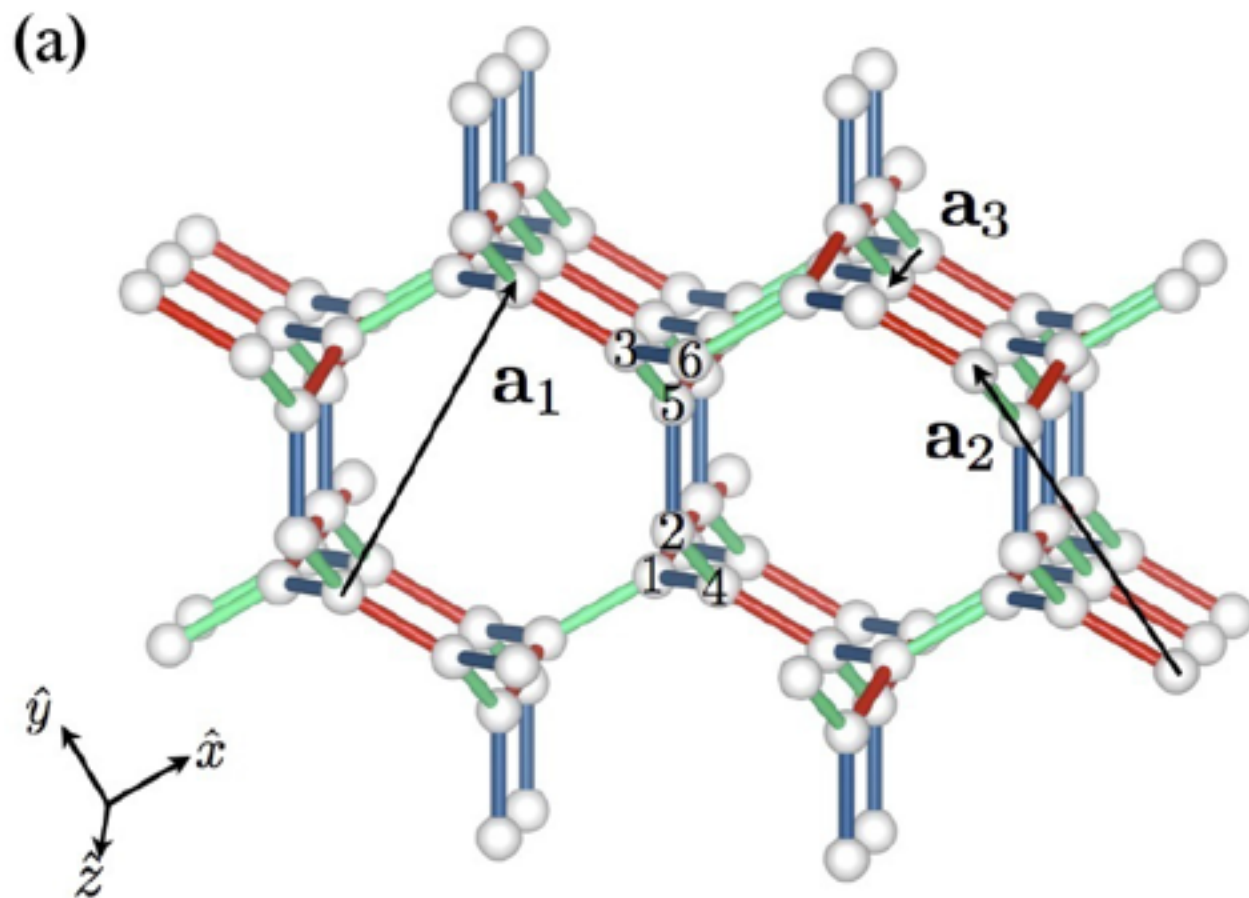


Hyperoctagon lattice Majorana metal

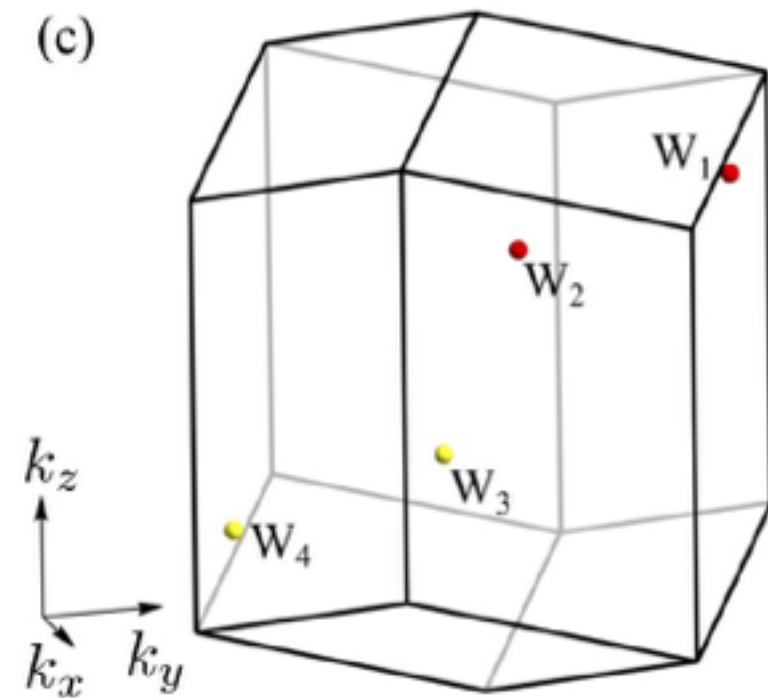
Fermi surfaces



Hyperhexagon lattice



gapless Weyl points



$$\hat{H}_{2 \times 2} = \mathbf{v}_0 \cdot \mathbf{q} \mathbb{1} + \sum_{j=1}^3 \mathbf{v}_j \cdot \mathbf{q} \sigma_j$$

Spectroscopy of Kitaev Spin Liquids

INS of Kitaev Spin Liquids (briefly)

Raman scattering in Kitaev Spin Liquids (briefly)

RIXS scattering in Kitaev Spin Liquids

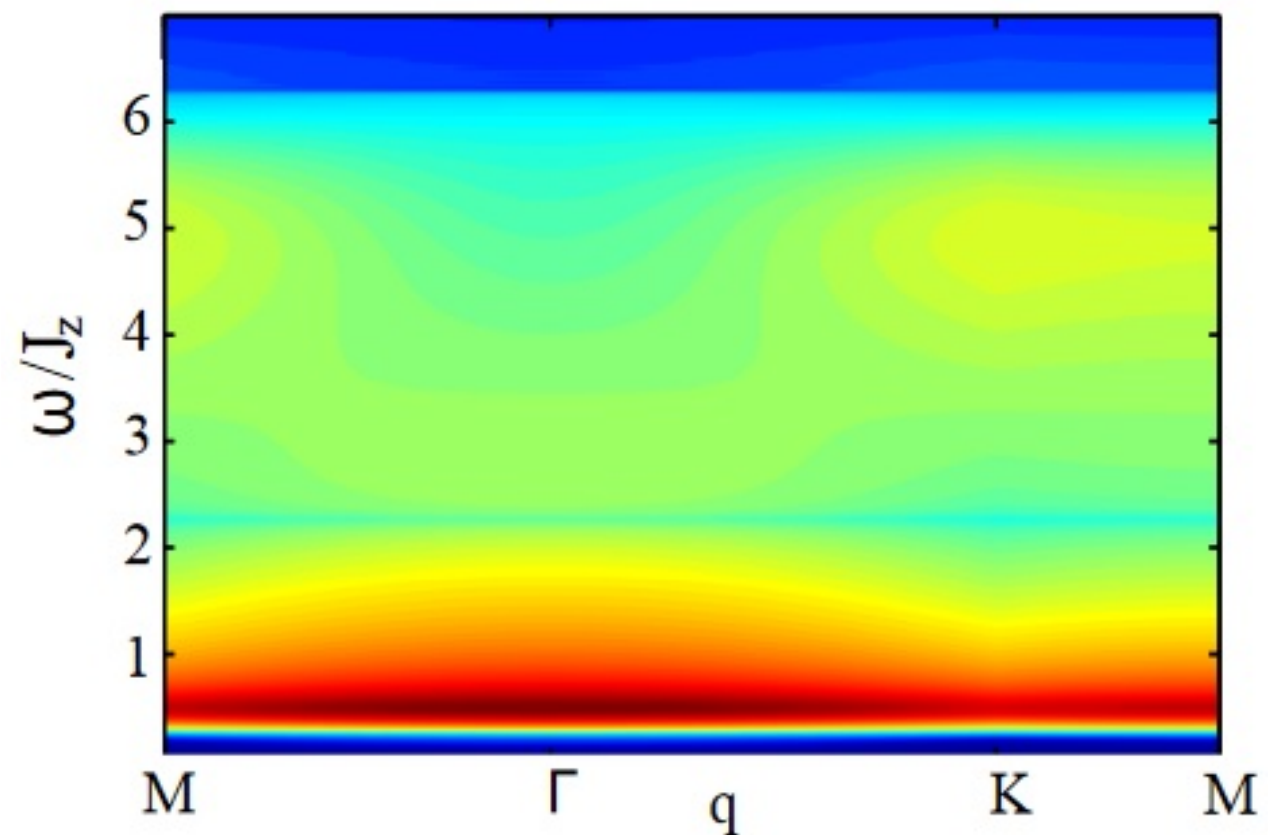
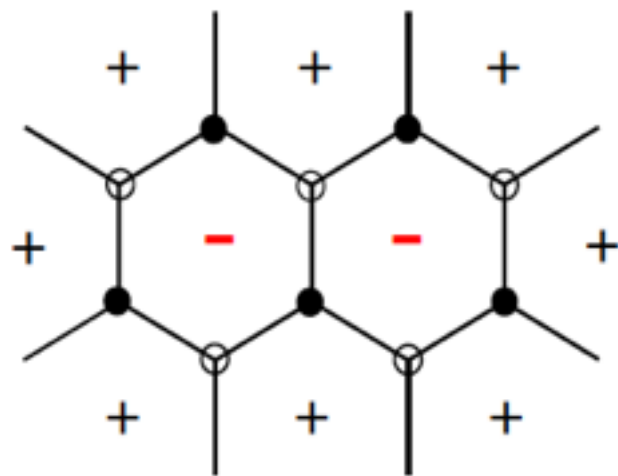
Inelastic neutron scattering of Kitaev Spin Liquids

QSL: expected spin-excitation continuum vs sharp dispersive features for spin-waves

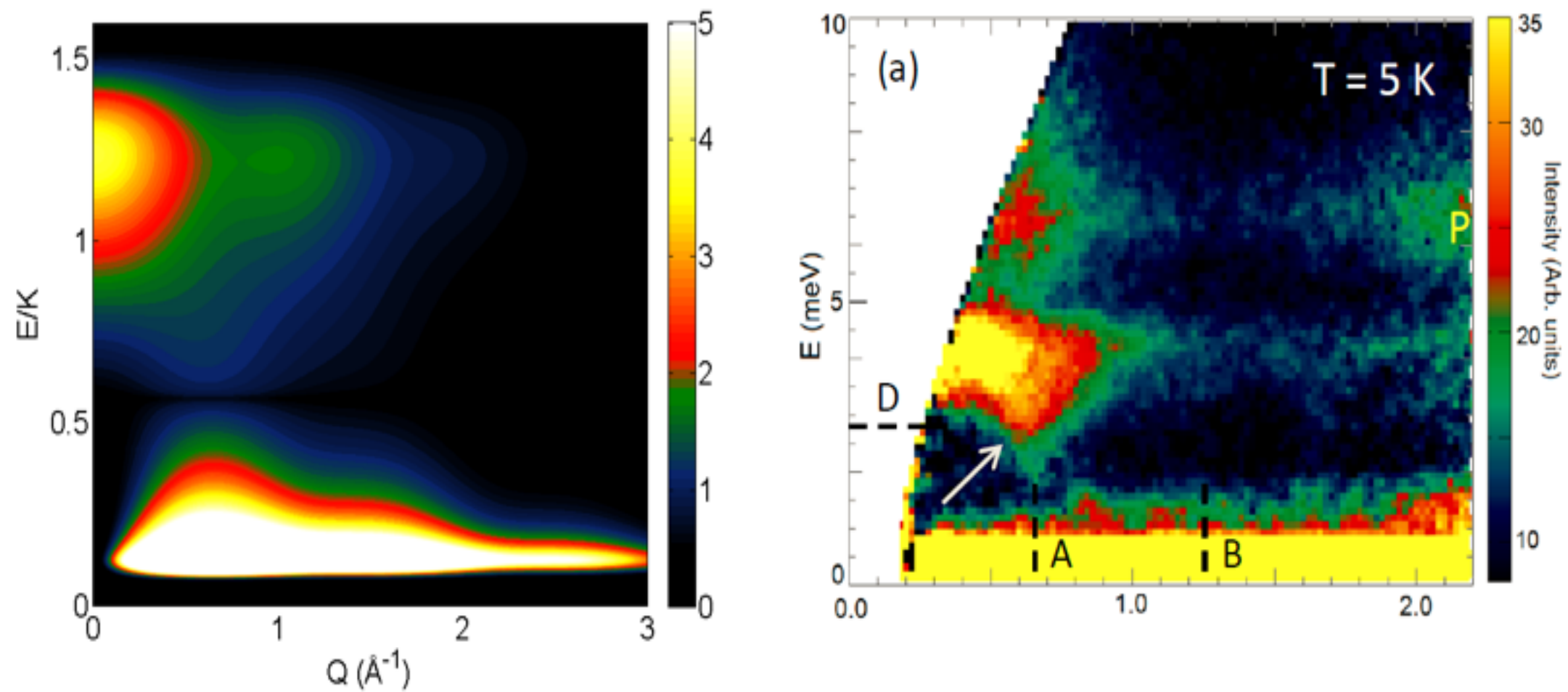
$$S_{\mathbf{q}}^{aa}(\omega) = \frac{1}{N} \sum_{ij} e^{-i\mathbf{q}(\mathbf{r}_i - \mathbf{r}_j)} \int_{-\infty}^{\infty} dt e^{i\omega t} S_{ij}^{aa}(t),$$

$$S_{ij}^{aa}(t) = \langle \hat{\sigma}_i^a(t) \hat{\sigma}_j^a(0) \rangle.$$

Measurement of a dynamic structure factor $S(\mathbf{q}, \omega)$ leads to a sudden insertion of a pair of Z_2 gauge-fluxes



RuCl_3

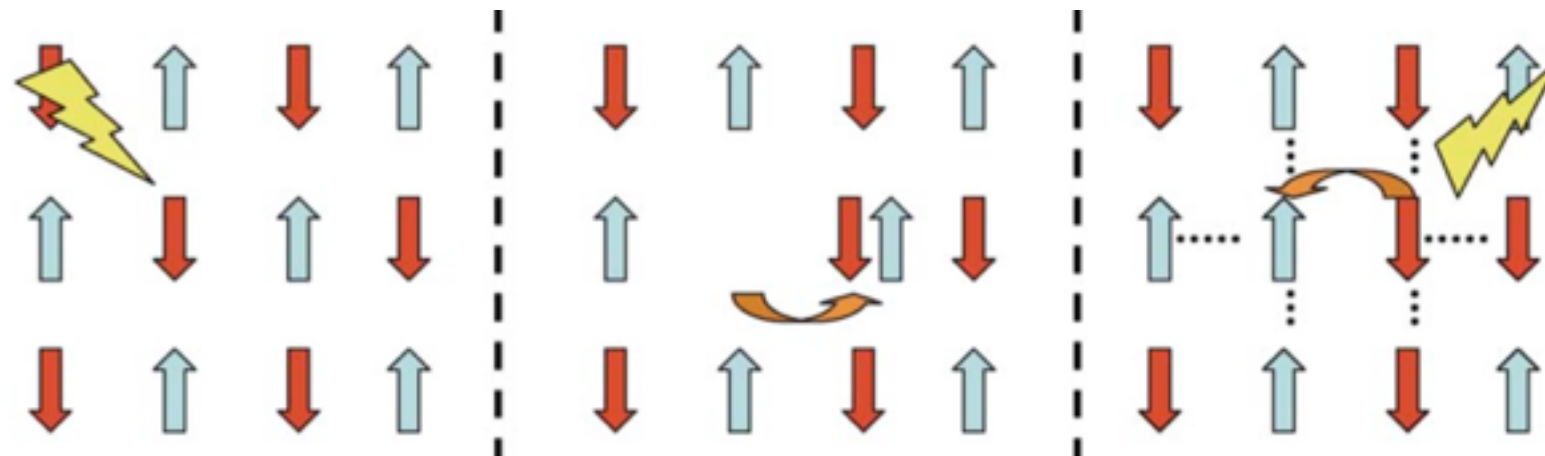


Signatures of fractionalization are visible!

Banerjee, et al., *Nature Mat.* (2016)
Banerjee, et al., *Science* (2017)

Raman spectroscopy of Kitaev Spin Liquids

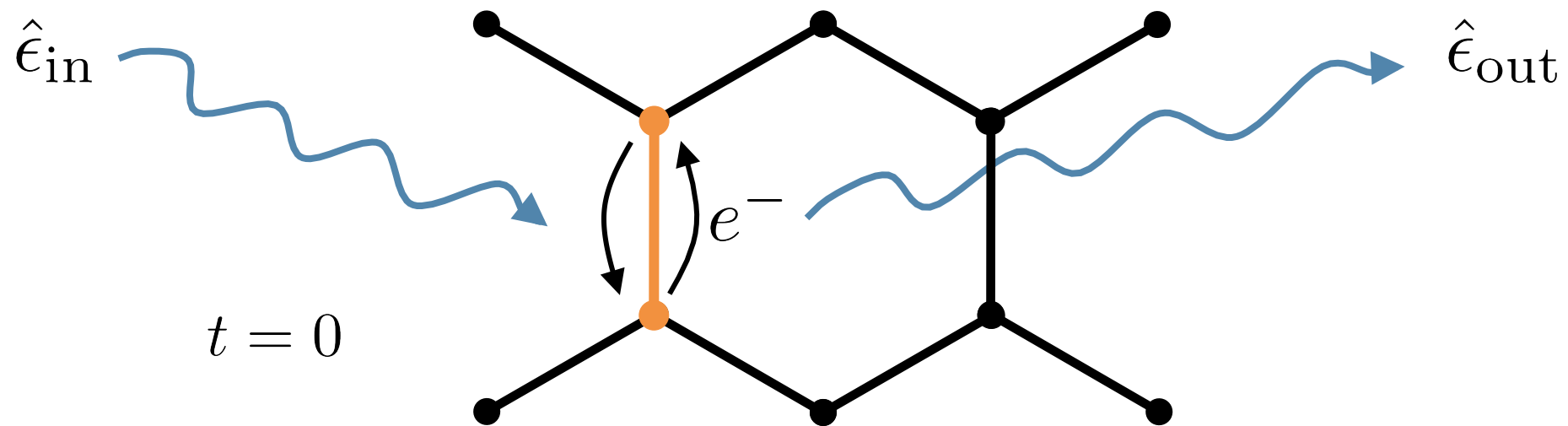
Photon-in photon-out process



Photon induced spin exchange

Raman Scattering in Kitaev model

$$I_{\text{Ram}}(\omega) \propto \int dt e^{i\omega t} \langle R e^{iHt} R \rangle$$

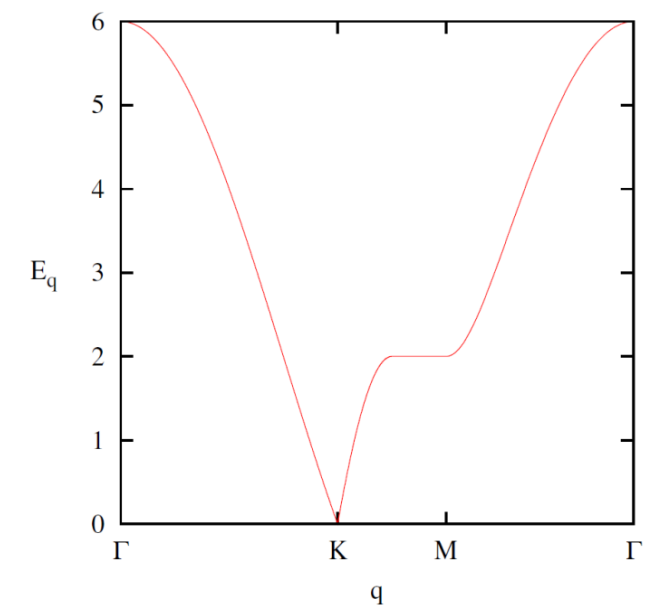
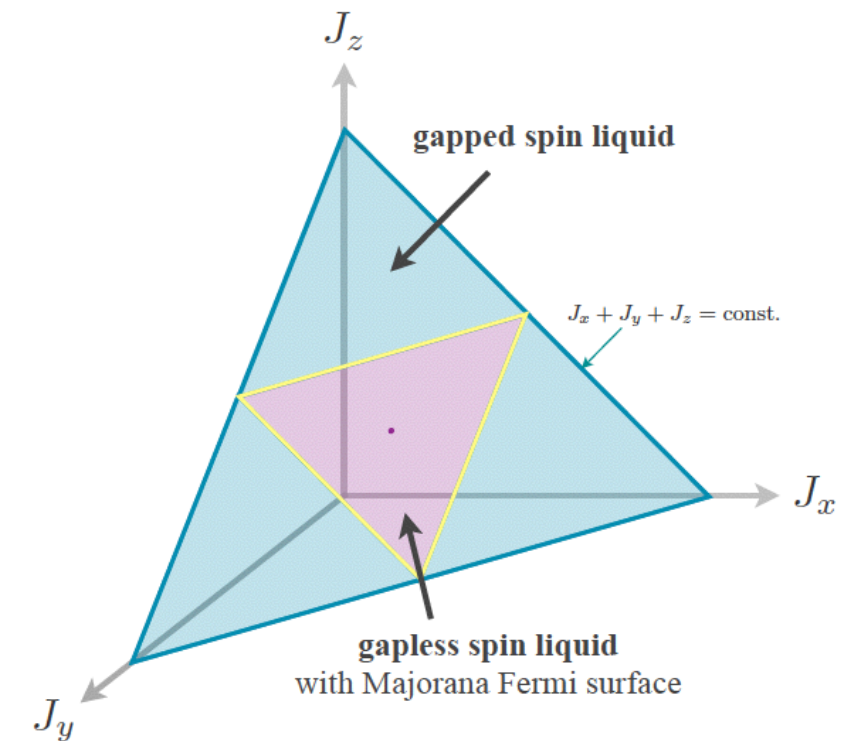
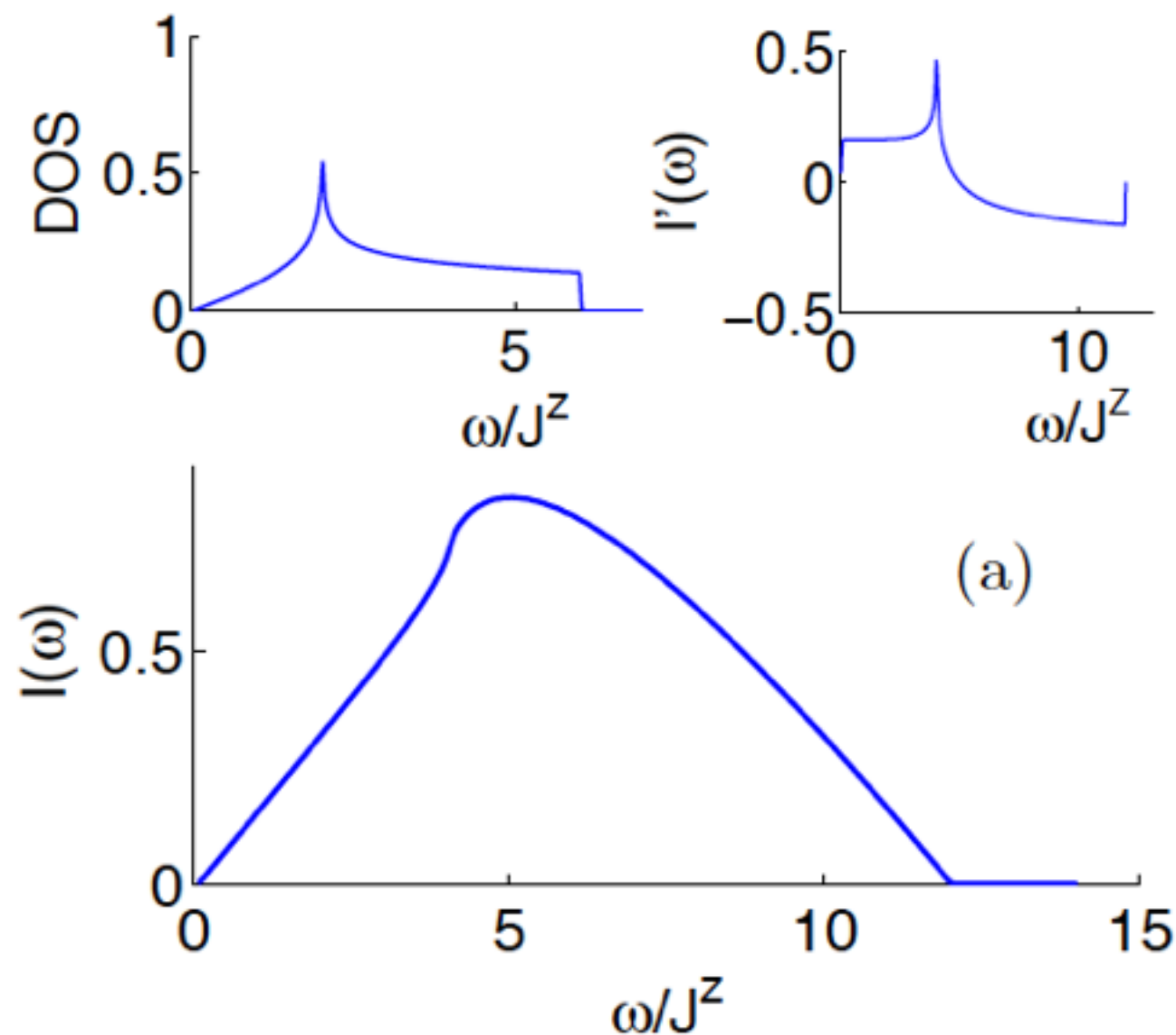


$$\begin{aligned}
 R &= \sum_{\langle ij \rangle^\alpha} (\epsilon_{\text{in}} \cdot \mathbf{d}^\alpha) (\epsilon_{\text{out}} \cdot \mathbf{d}^\alpha) J^\alpha \sigma_i^\alpha \sigma_j^\alpha \\
 &= i \sum_{\langle ij \rangle^\alpha} (\epsilon_{\text{in}} \cdot \mathbf{d}^\alpha) (\epsilon_{\text{out}} \cdot \mathbf{d}^\alpha) J^\alpha u_{\langle ij \rangle^\alpha} c_i c_j
 \end{aligned}$$

Raman vertex: diagonal in fluxes but creates two Majorana fermions

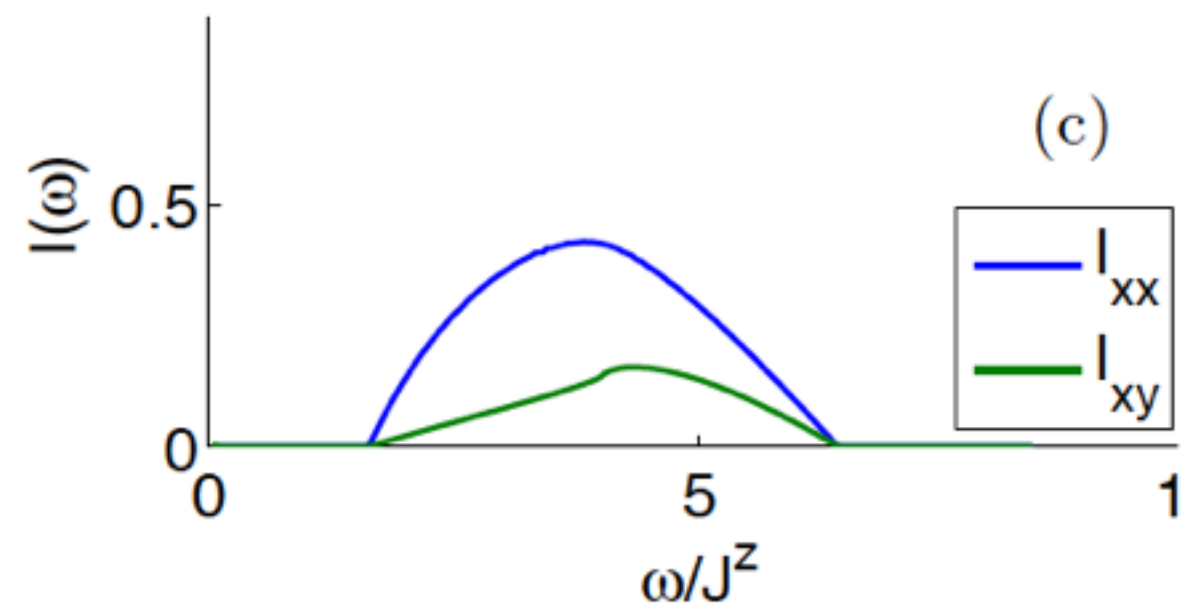
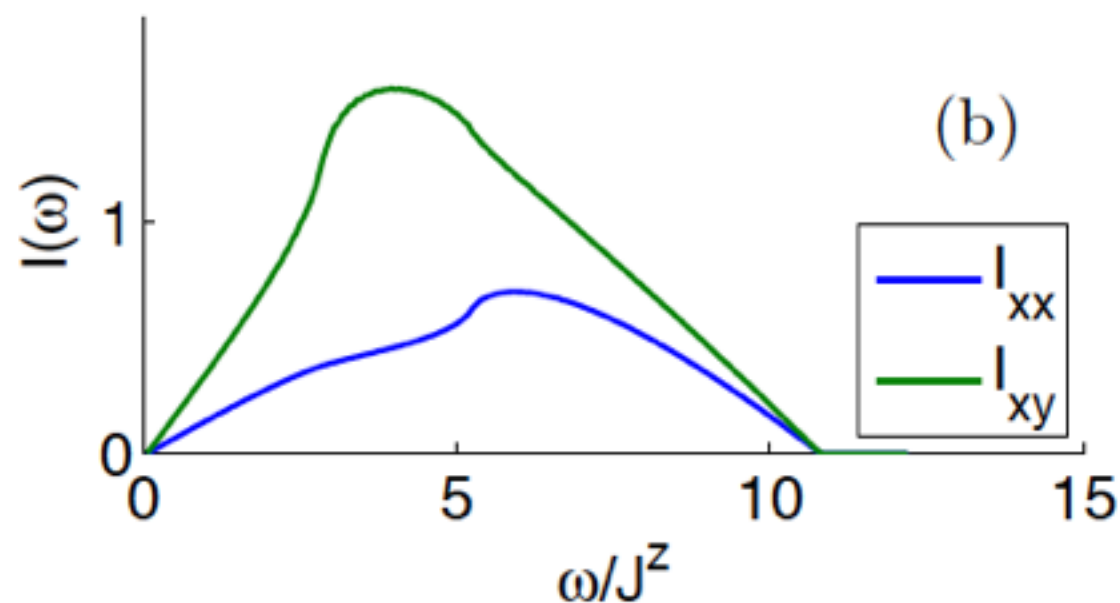
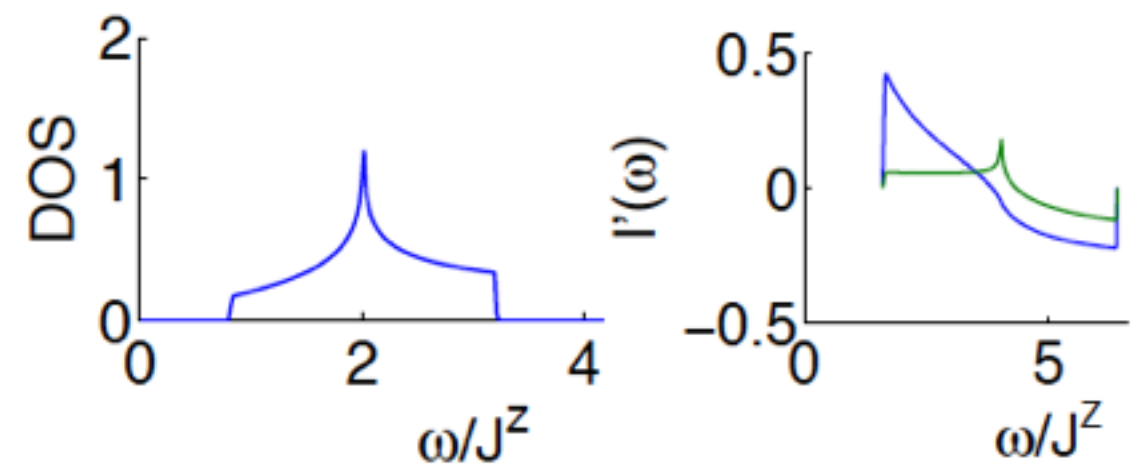
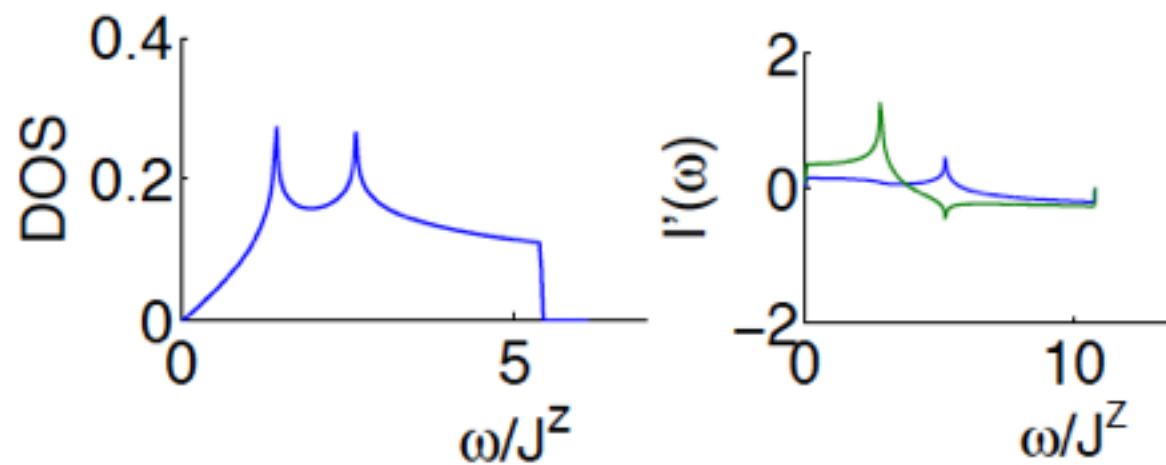
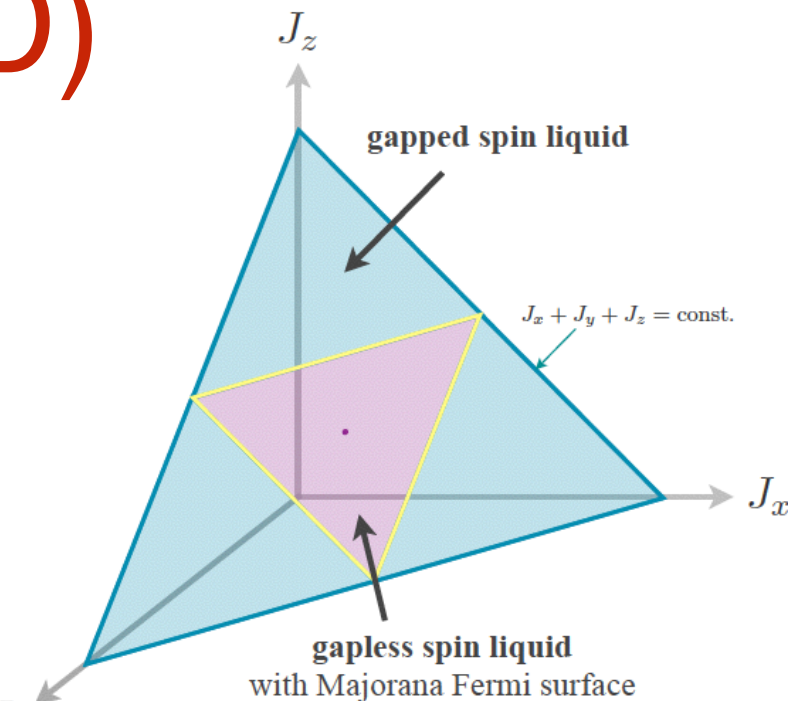
Raman Scattering results (2D)

isotropic point:
polarization independent



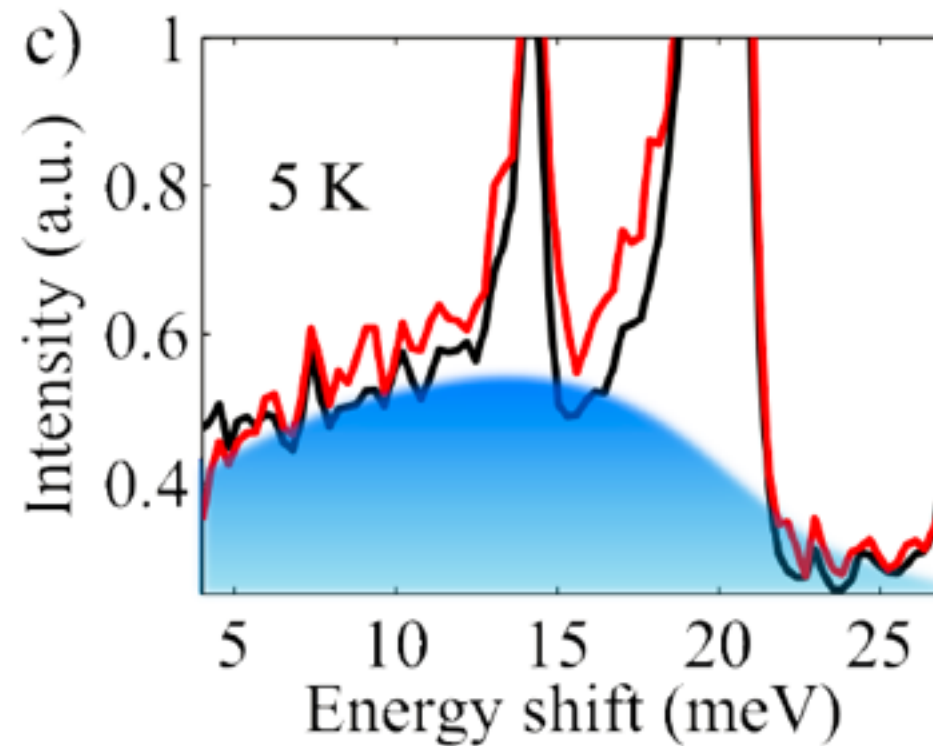
Raman Scattering results (2D)

anisotropic point:
polarization dependence



RuCl_3

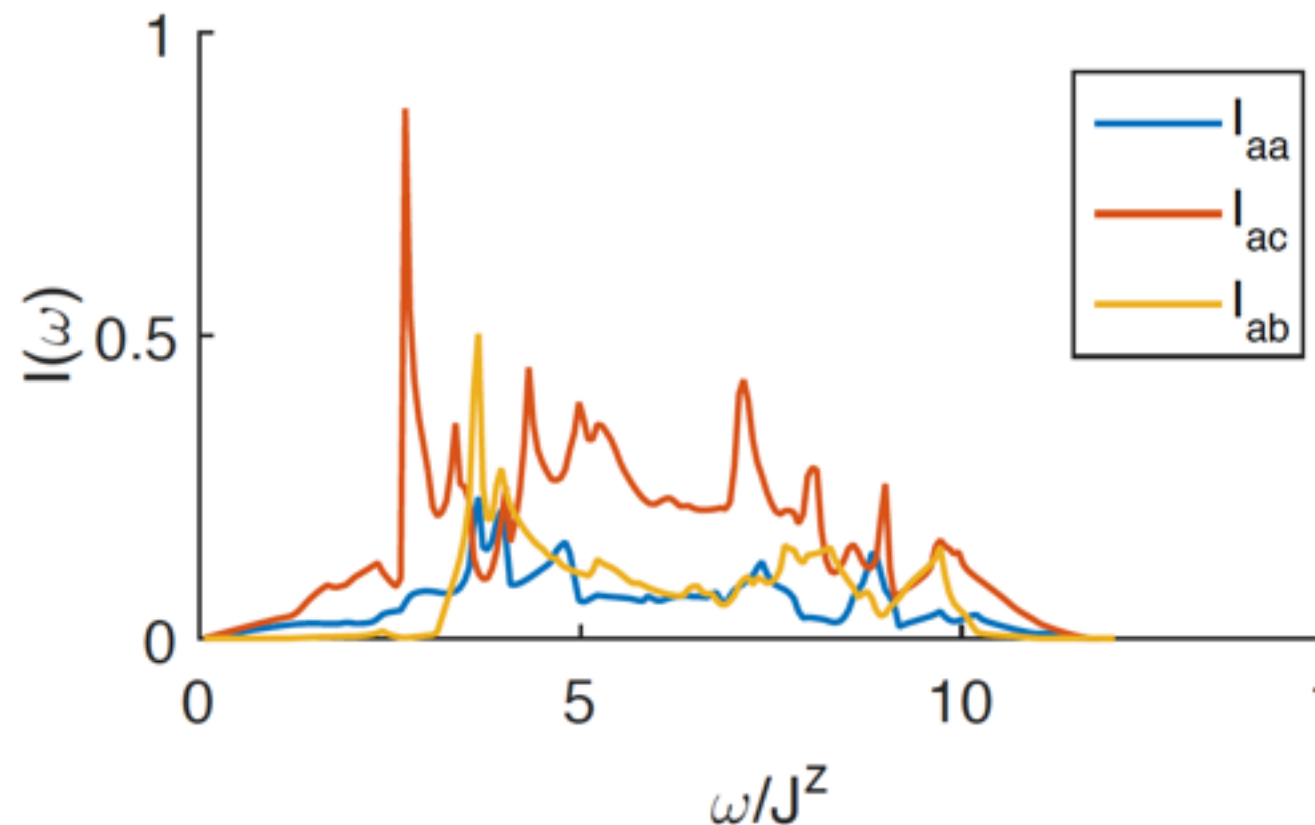
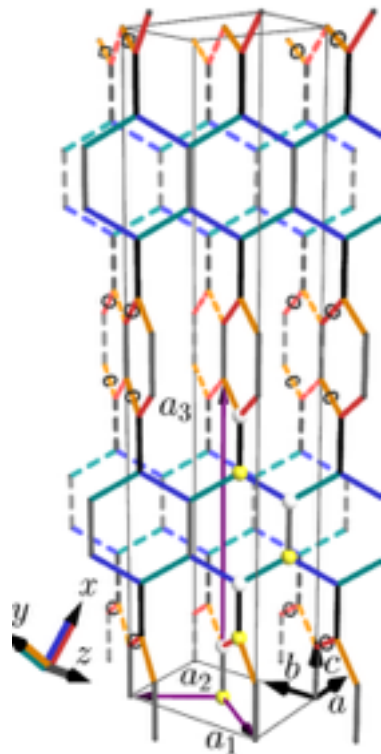
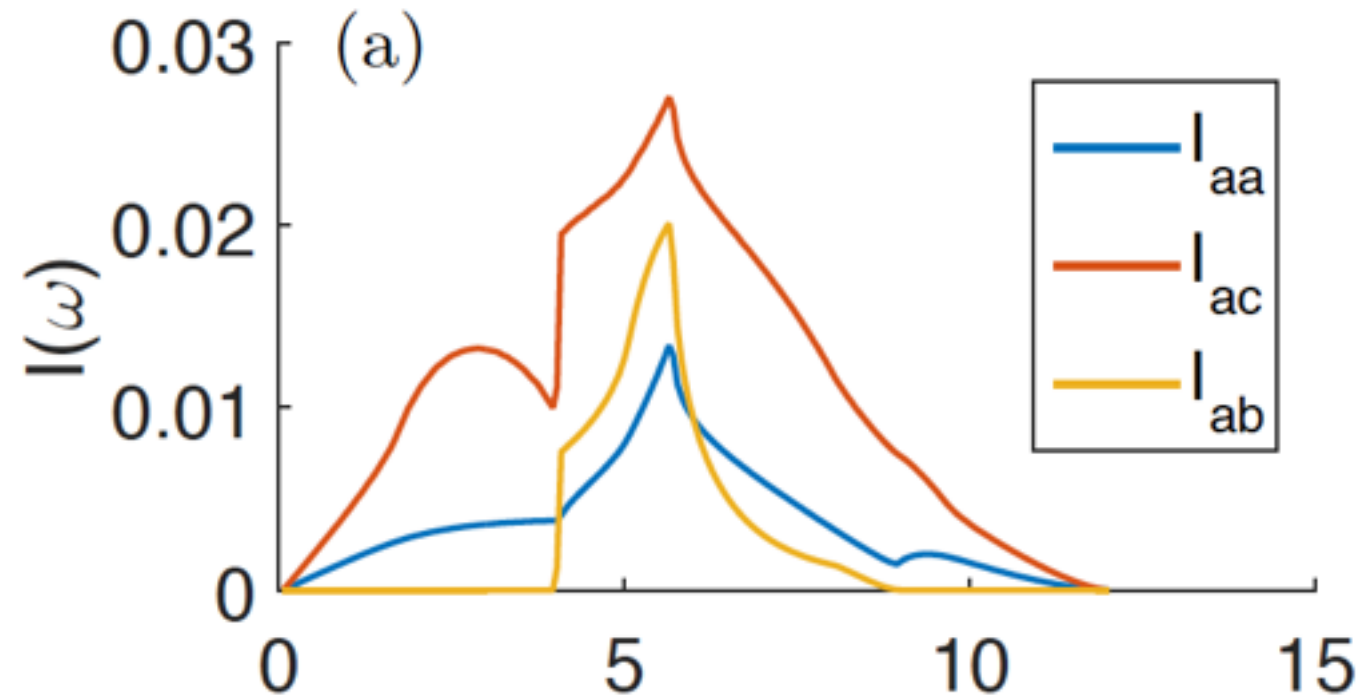
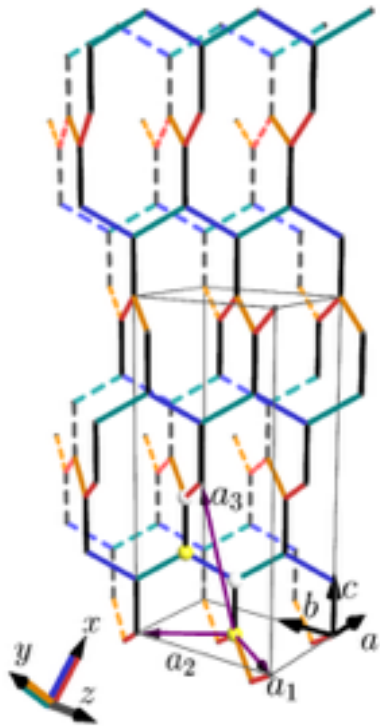
L. Sandilands, Y.J. Kim, K.S. Burch
Phys. Rev. Lett. 114 (2015)



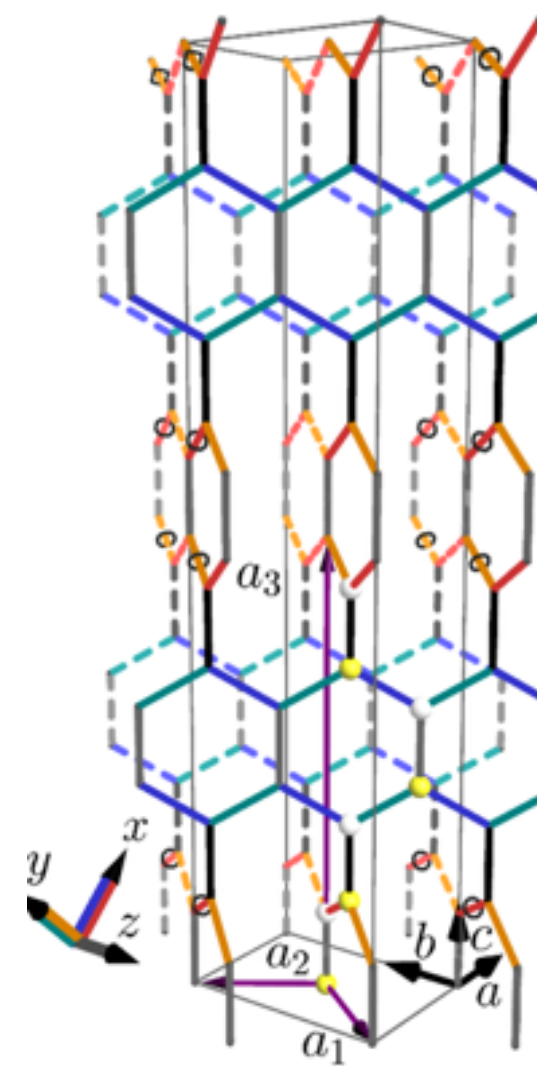
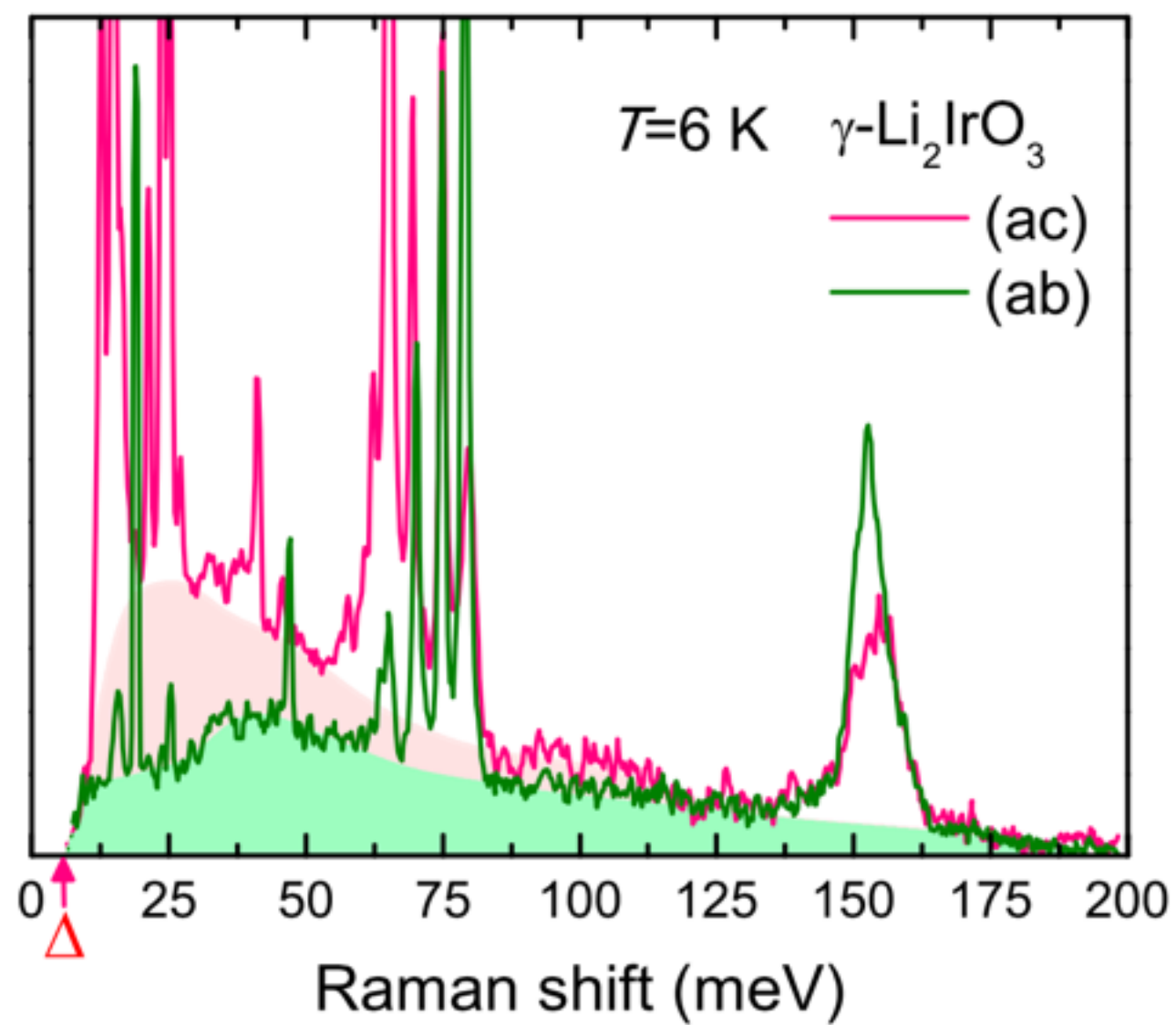
Big 'hump' with fine features of the Majorana DOS.
Signatures of fractionalization are visible!
(comparison gives $J_K \sim 8 \text{ meV}$)

Raman Scattering results (3D)

The Raman response is polarization dependent!

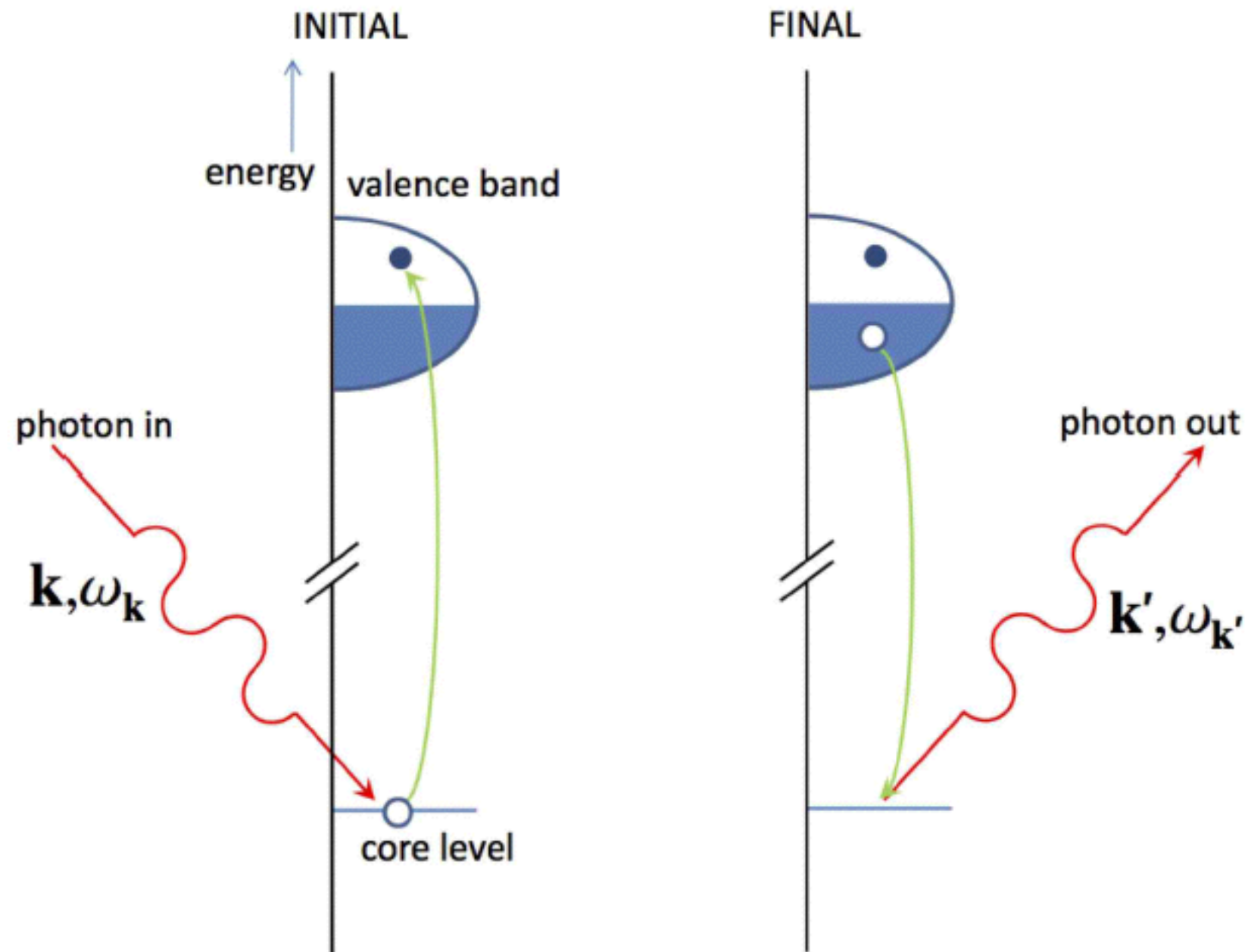


γ -Li₂IrO₃



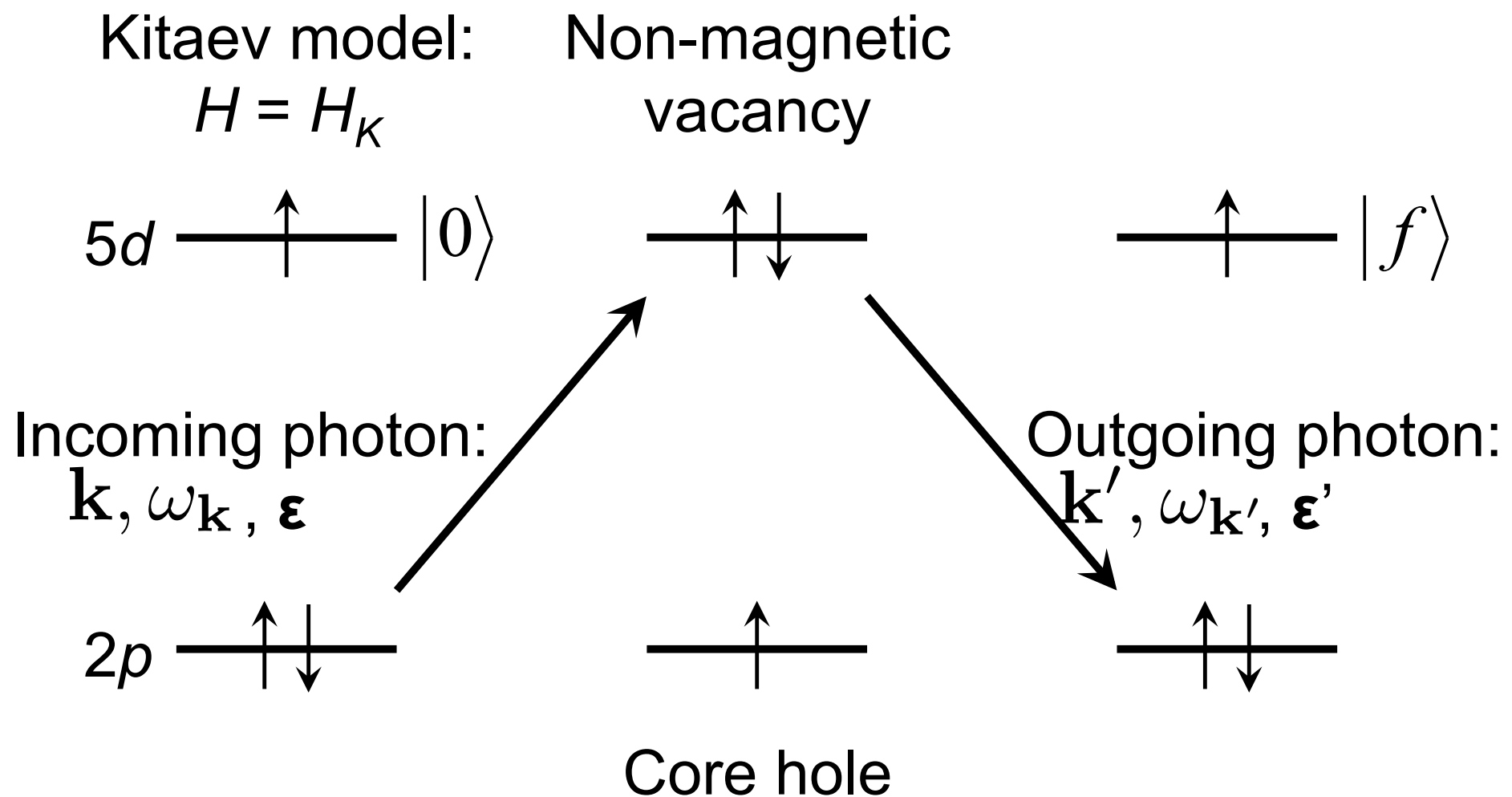
Glamazda, Lemmens, Do, Choi, Choi, Nature Comm. 7 (2016)

RIXS spectroscopy of Kitaev Spin Liquids

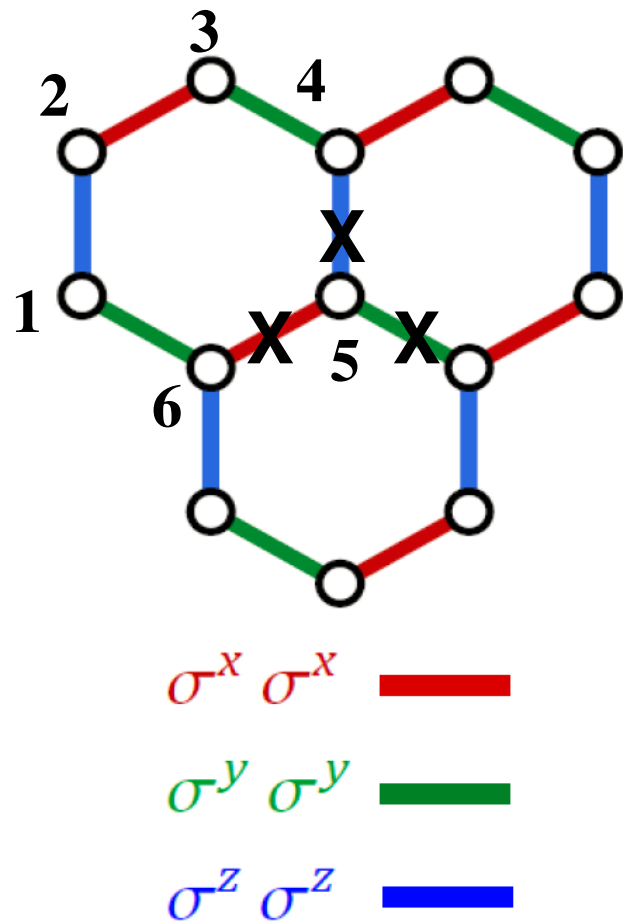


RIXS from Ir⁴⁺

(Na,Li)₂IrO₃ with Ir⁴⁺ in 5d⁵ configuration [*L*₃ edge]:



Intermediate state with a vacancy



The Kitaev model with a single vacancy at site \mathbf{r}
 = the original Kitaev model with switched off
 couplings around site \mathbf{r} (**exactly solvable**)

Description: the vacancy is always in the spin-up
 state and the couplings to NN are zero.

$$d_{\mathbf{r},\downarrow}^\dagger \rightarrow \frac{1}{2} (1 + \sigma_{\mathbf{r}}^z), \quad d_{\mathbf{r},\uparrow}^\dagger \rightarrow \frac{1}{2} \sigma_{\mathbf{r}}^x (1 - \sigma_{\mathbf{r}}^z)$$

$$d_{\mathbf{r},\downarrow}^\dagger |\uparrow\rangle = |\uparrow\rangle$$

$$d_{\mathbf{r},\uparrow}^\dagger |\uparrow\rangle = 0$$

$$d_{\mathbf{r},\downarrow}^\dagger |\downarrow\rangle = 0$$

$$d_{\mathbf{r},\uparrow}^\dagger |\downarrow\rangle = |\uparrow\rangle$$

RIXS amplitude for the Kitaev model

$$I(\omega, \mathbf{q}) = \sum_m \left| \sum_{\alpha, \beta} T_{\alpha\beta} A_{\alpha\beta}(m, \mathbf{q}) \right|^2 \delta(\omega - E_m)$$

$$A_{\alpha\beta}(m, \mathbf{q}) = \sum_{\mathbf{r}, \tilde{n}_{\mathbf{r}}} \frac{\langle m | d_{\mathbf{r}, \alpha} | \tilde{n}_{\mathbf{r}} \rangle \langle \tilde{n}_{\mathbf{r}} | d_{\mathbf{r}, \beta}^\dagger | 0 \rangle}{\Omega - E_{\tilde{n}} + i\Gamma} e^{i\mathbf{q} \cdot \mathbf{r}}$$

$$\mathbf{q} \equiv \mathbf{k} - \mathbf{k}'$$

Kramers–Heisenberg formula

The four fundamental RIXS channels are introduced by decomposing the polarization tensor into

$$T_{\alpha\beta} = P_\eta \sigma_{\alpha\beta}^\eta$$

(a) Spin-conserving (SC) channel with $T_{\alpha\beta} \propto \sigma_{\alpha\beta}^0$

$$P_0 = \epsilon'^* \cdot \epsilon$$

(b) three non spin-conserving (NSC) channels with $T_{\alpha\beta} \propto \sigma_{\alpha\beta}^{x,y,z}$

$$P_x = i(\epsilon'_y{}^* \epsilon_z - \epsilon'_z{}^* \epsilon_y)$$

and cyclic permutations

The four fundamental RIXS channels

$$A(m, \mathbf{q}) = \sum_{\nu} P_{\nu} A_{\nu}(m, \mathbf{q})$$

$$A_{\nu}(m, \mathbf{q}) = \sum_{\mathbf{r}} e^{i\mathbf{q}\mathbf{r}} e^{-\Gamma t} \langle m | \sigma_{\mathbf{r}}^{\nu} e^{-it\tilde{H}_{\mathbf{r}}} | 0 \rangle$$

Spin-conserving (SC) channel:

$$A_0(m, \mathbf{q}) = \sum_{\mathbf{r}} e^{i\mathbf{q}\mathbf{r}} e^{-\Gamma t} \langle m | e^{-it\tilde{H}_{\mathbf{r}}} | 0 \rangle$$

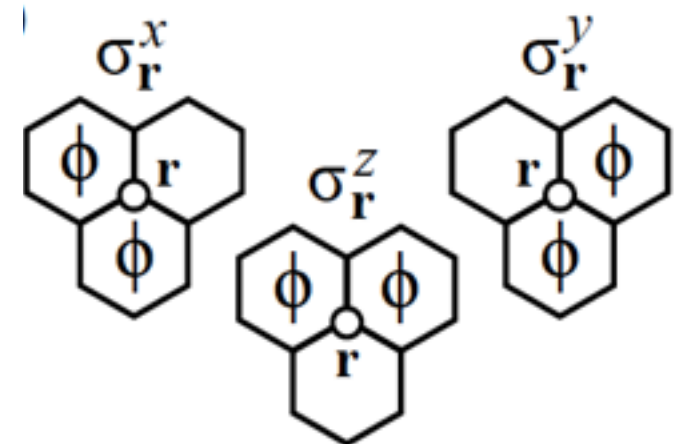
Three non spin-conserving (NSC) channels:

$$A_x(m, \mathbf{q}) = \sum_{\mathbf{r}} e^{i\mathbf{q}\mathbf{r}} e^{-\Gamma t} \langle m | \sigma_{\mathbf{r}}^x e^{-it\tilde{H}_{\mathbf{r}}} | 0 \rangle$$

$$A_y(m, \mathbf{q}) = \sum_{\mathbf{r}} e^{i\mathbf{q}\mathbf{r}} e^{-\Gamma t} \langle m | \sigma_{\mathbf{r}}^y e^{-it\tilde{H}_{\mathbf{r}}} | 0 \rangle$$

$$A_z(m, \mathbf{q}) = \sum_{\mathbf{r}} e^{i\mathbf{q}\mathbf{r}} e^{-\Gamma t} \langle m | \sigma_{\mathbf{r}}^z e^{-it\tilde{H}_{\mathbf{r}}} | 0 \rangle$$

create two flux excitations



Fast collision approximation

$$(\text{Na,Li})_2\text{IrO}_3 \text{ and } \alpha\text{-RuCl}_3 : \Gamma / J_{x,y,z} \gg 1$$

$$t \sim 1 / \Gamma \ll 1 / J_{x,y,z} \rightarrow$$

The lowest order RIXS amplitude is then

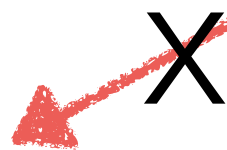
$$\begin{aligned} A_\eta(m, \mathbf{q}) &\propto \sum_{\mathbf{r}} e^{i\mathbf{q}\cdot\mathbf{r}} \langle m | \sigma_{\mathbf{r}}^\eta \left[1 - \frac{i\tilde{H}(\mathbf{r})}{\Gamma} \right] | 0 \rangle \\ &= \sum_{\mathbf{r}} e^{i\mathbf{q}\cdot\mathbf{r}} \langle m | \sigma_{\mathbf{r}}^\eta \left[1 - \frac{i}{\Gamma} \sum_{\kappa} J_\kappa \sigma_{\mathbf{r}}^\kappa \sigma_{\kappa(\mathbf{r})}^\kappa \right] | 0 \rangle \end{aligned}$$

NSC channels recover INS amplitudes for infinite Γ

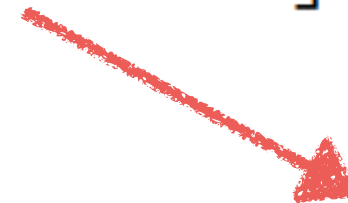
Flux creation: Finite gap, little dispersion

Results: SC channel 2D Kitaev model

$$A_0(m, \mathbf{q}) \propto \sum_{\mathbf{r}} e^{i\mathbf{q} \cdot \mathbf{r}} \langle m | \left[1 - \frac{i}{\Gamma} \sum_{\kappa=x,y,z} J_{\kappa} \sigma_{\mathbf{r}}^{\kappa} \sigma_{\kappa(\mathbf{r})}^{\kappa} \right] | 0 \rangle$$



Elastic response



Inelastic response

$|m\rangle \neq |0\rangle$

no flux and two fermion excitations

$$\omega = \varepsilon_{\mathbf{k}} + \varepsilon_{\mathbf{q}-\mathbf{k}}$$

$$I_0(\omega, \mathbf{q}) = \sum_m |A_0(m, \mathbf{q})|^2 \delta(\omega - E_m)$$

$$I_0(\omega, \mathbf{q}) \propto \int_{\text{BZ}} d^2\mathbf{k} \delta(\omega - \varepsilon_{\mathbf{k}} - \varepsilon_{\mathbf{q}-\mathbf{k}}) [\varepsilon_{\mathbf{k}} - \varepsilon_{\mathbf{q}-\mathbf{k}}]^2 \left| 1 - e^{i\varphi_{\mathbf{k}}} e^{i\varphi_{\mathbf{q}-\mathbf{k}}} \right|^2$$



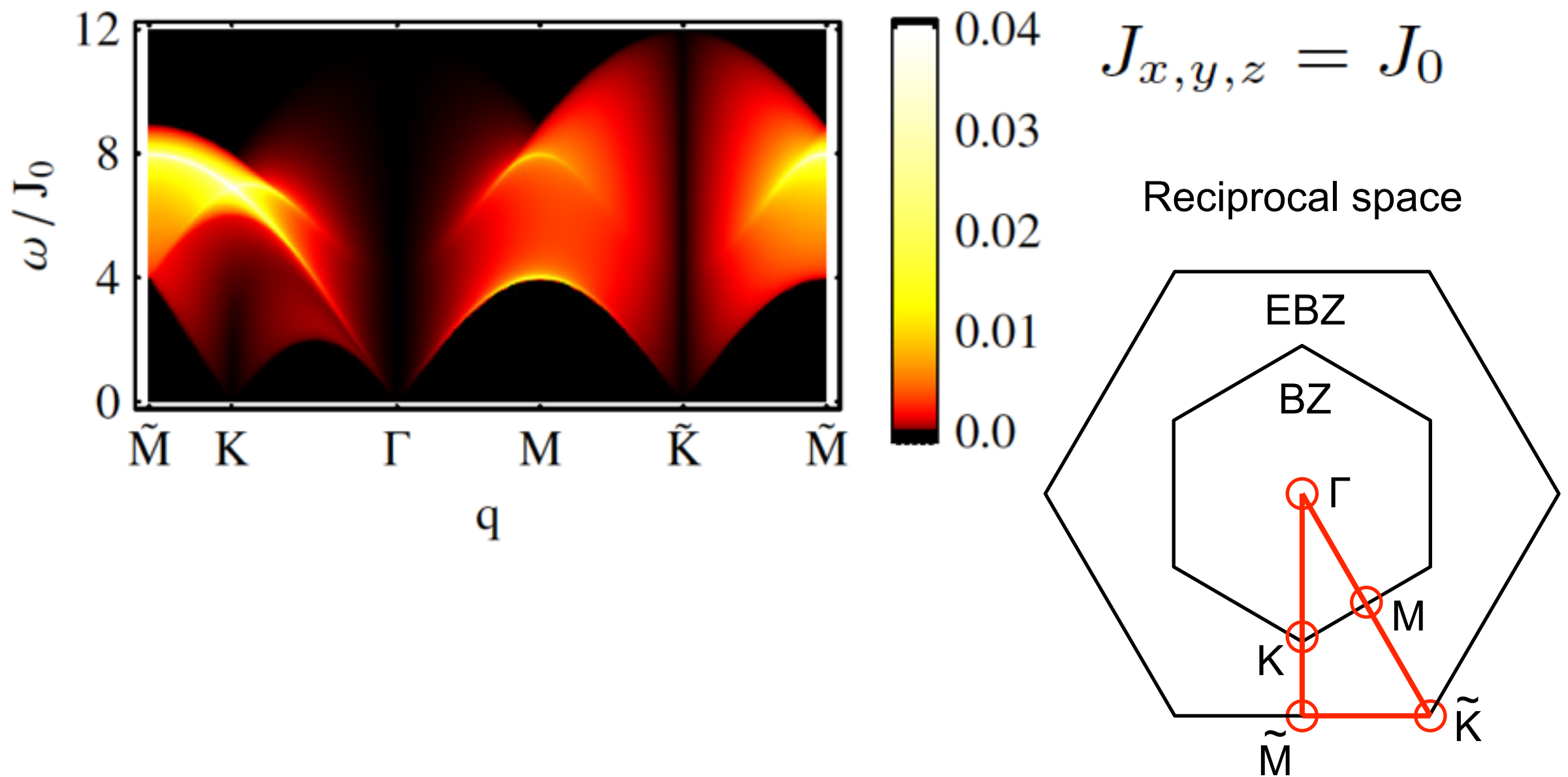
A



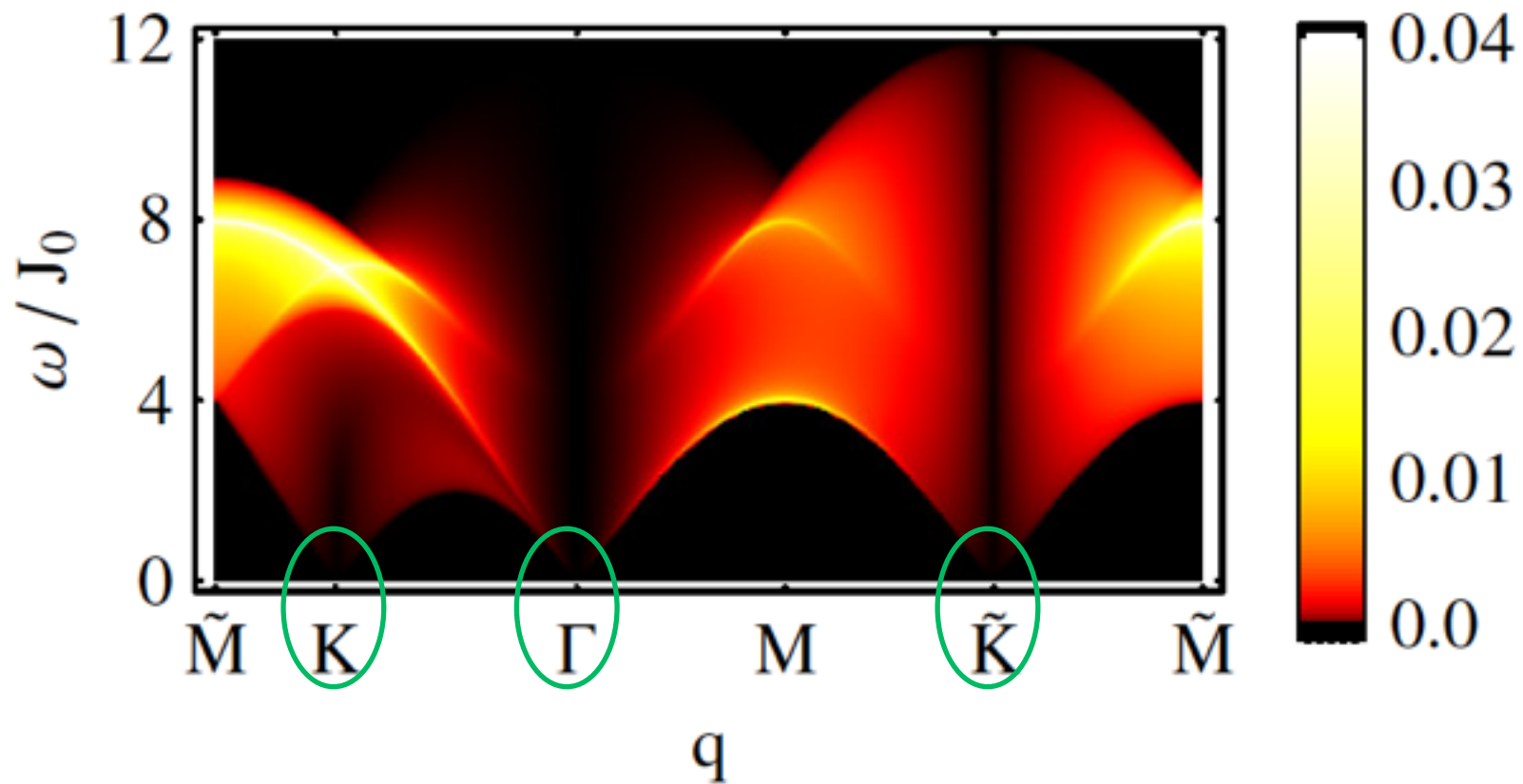
B

interference between the two sublattices

RIXS response in SC channel

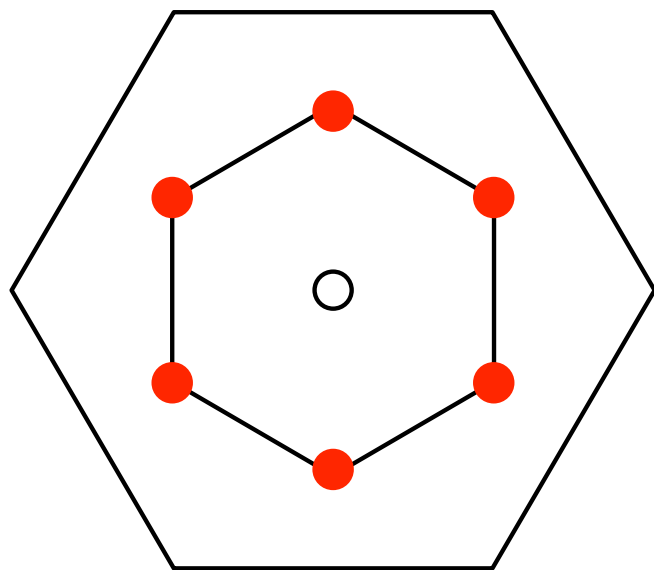


RIXS response in SC channel



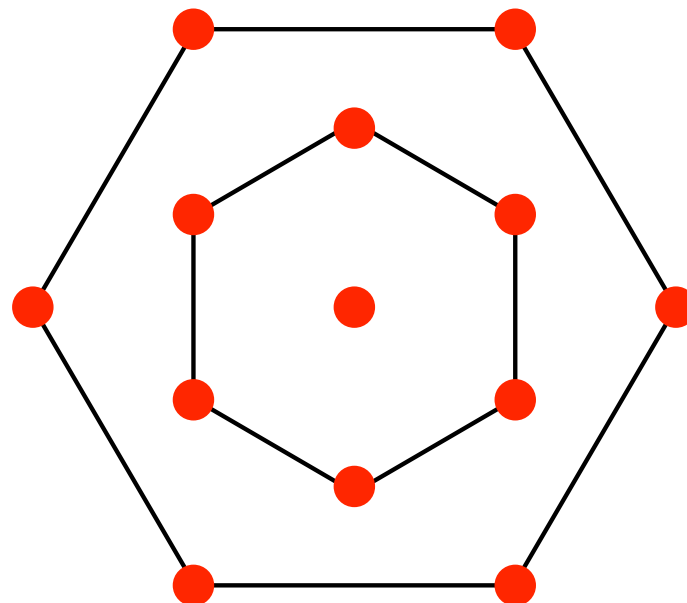
Gapless response at a finite number of discrete points

Dirac points



K points

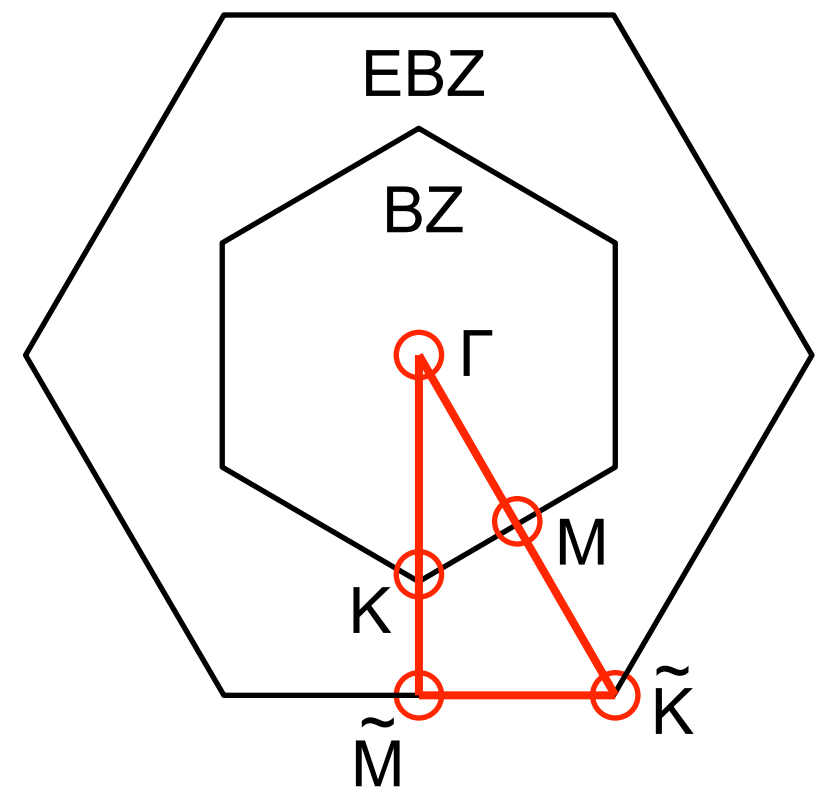
Gapless points



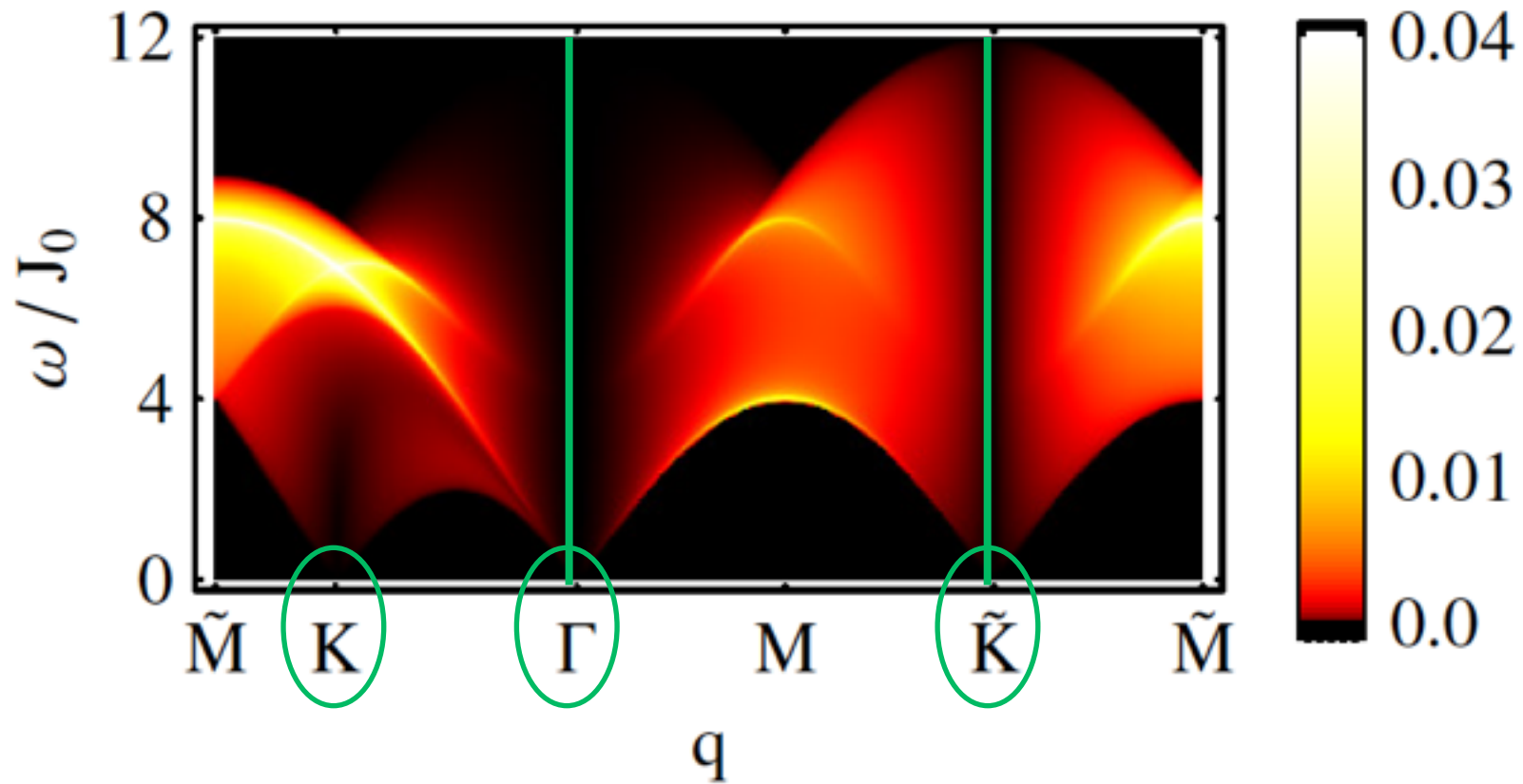
Γ , K, \tilde{K} points

$$J_{x,y,z} = J_0$$

Reciprocal space



RIXS response in SC channel

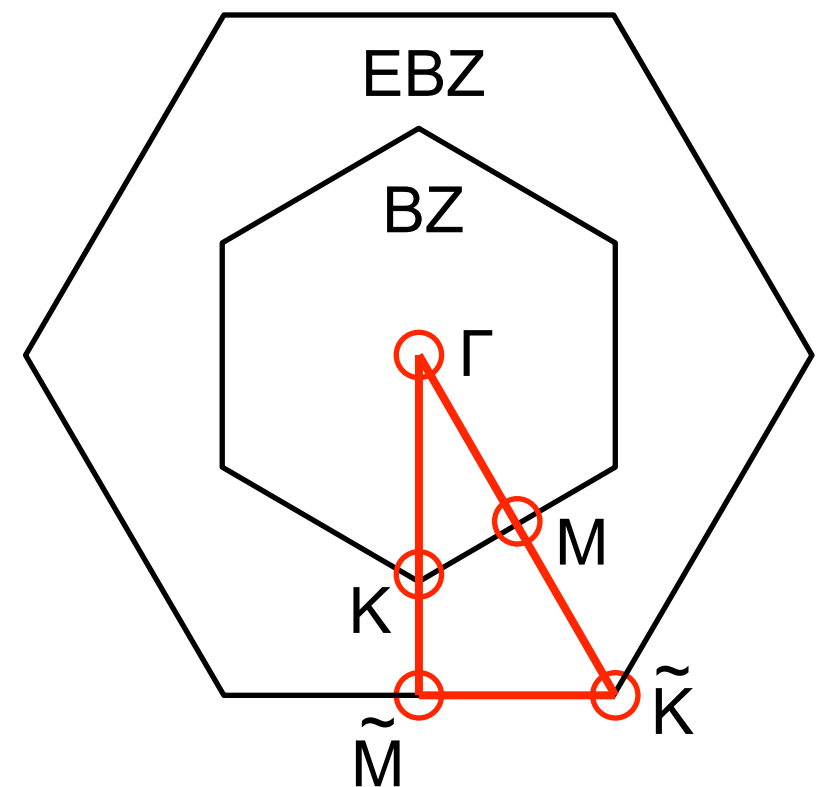


the response actually vanishes at the Γ and \tilde{K} points due to the factor

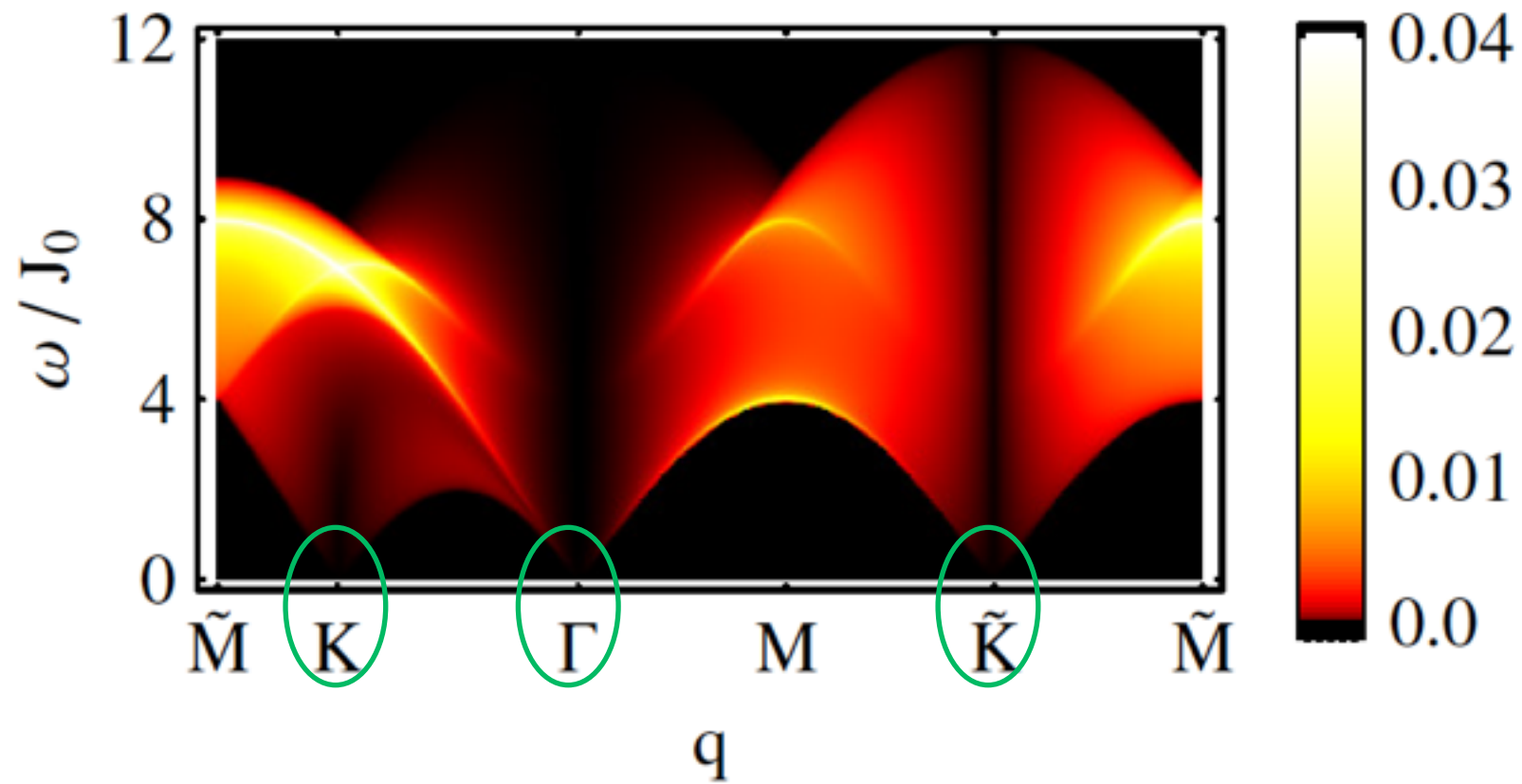
$$\tilde{I}_0(\mathbf{k}, \mathbf{q}) \propto [\varepsilon_{\mathbf{k}} - \varepsilon_{\mathbf{q}-\mathbf{k}}]^2$$

$$J_{x,y,z} = J_0$$

Reciprocal space

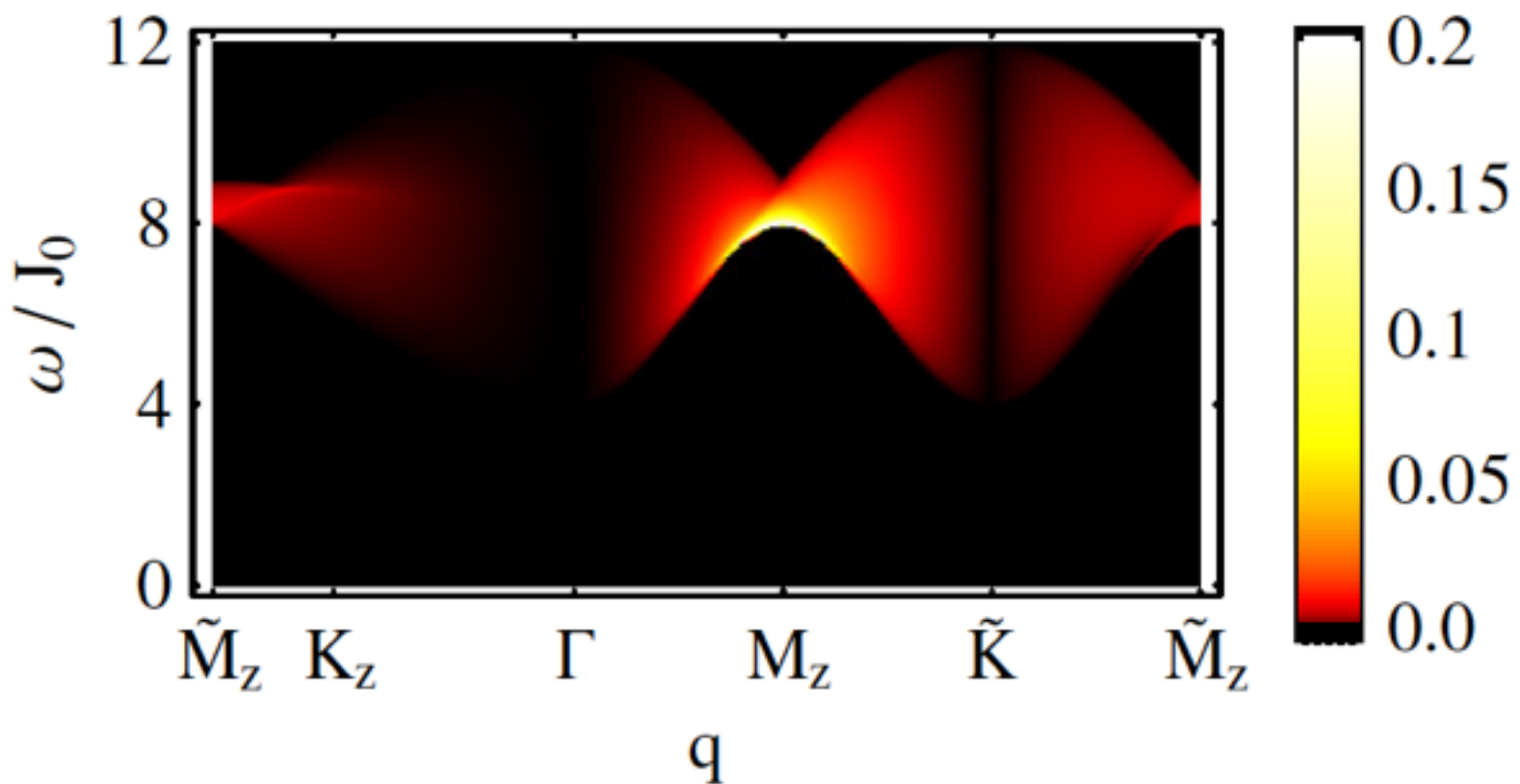
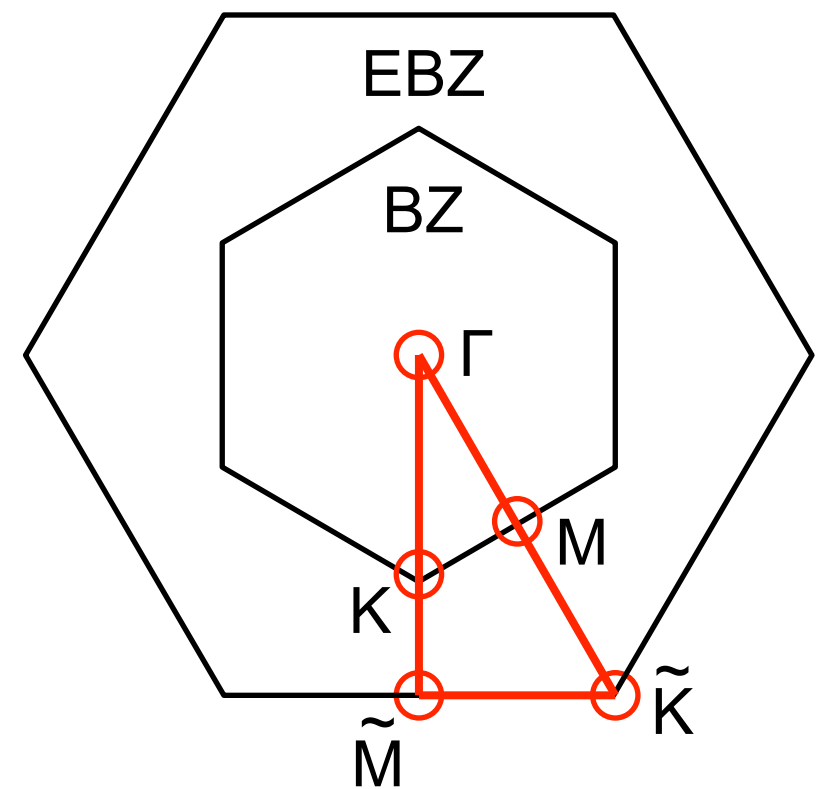


RIXS response in SC channel



$$J_{x,y,z} = J_0$$

Reciprocal space



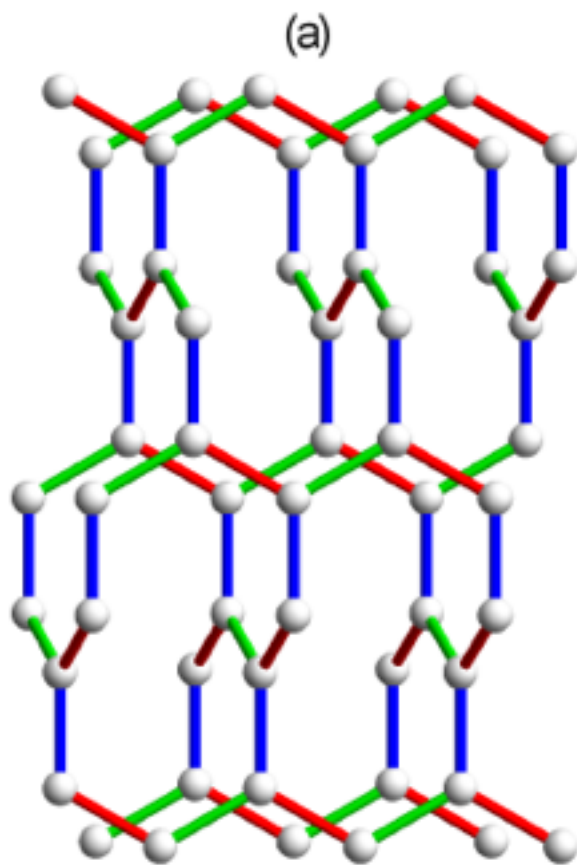
$$J_{x,y} = J_0/2$$

$$J_z = 2J_0$$

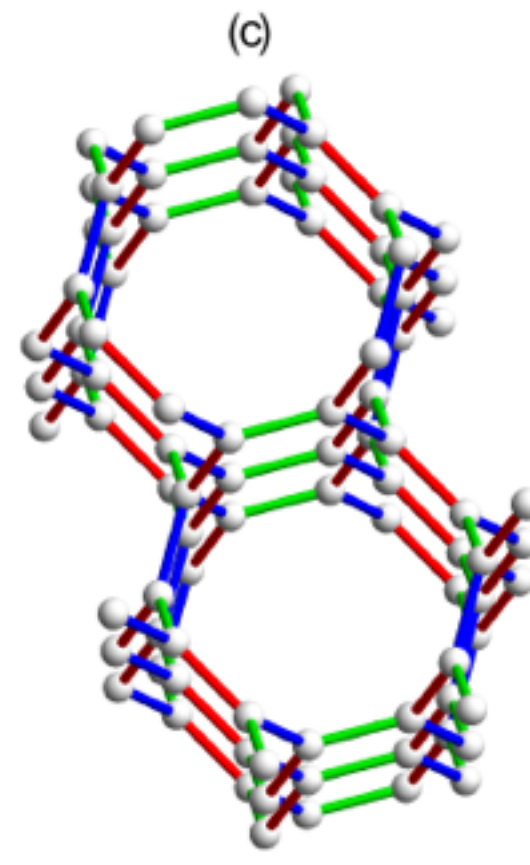
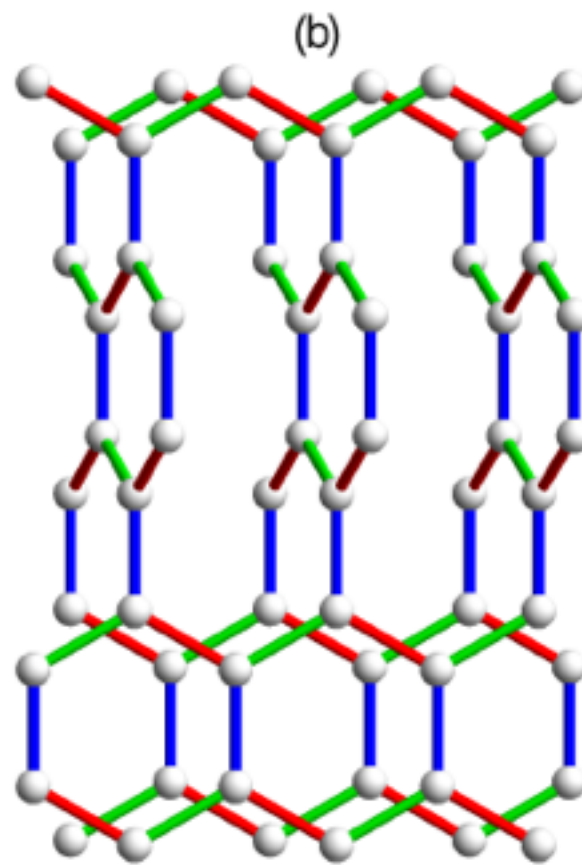
Results: SC channel in 3D Kitaev models

$$I_0(\omega, \mathbf{q}) \propto \sum_{\mathbf{k}, \mu, \mu'} |(\mathcal{A}_{\mathbf{q}, \mathbf{k}})_{\mu\mu'}|^2 \delta(\omega - \varepsilon_{\mathbf{k}, \mu} - \varepsilon_{\mathbf{q}-\mathbf{k}, \mu'})$$

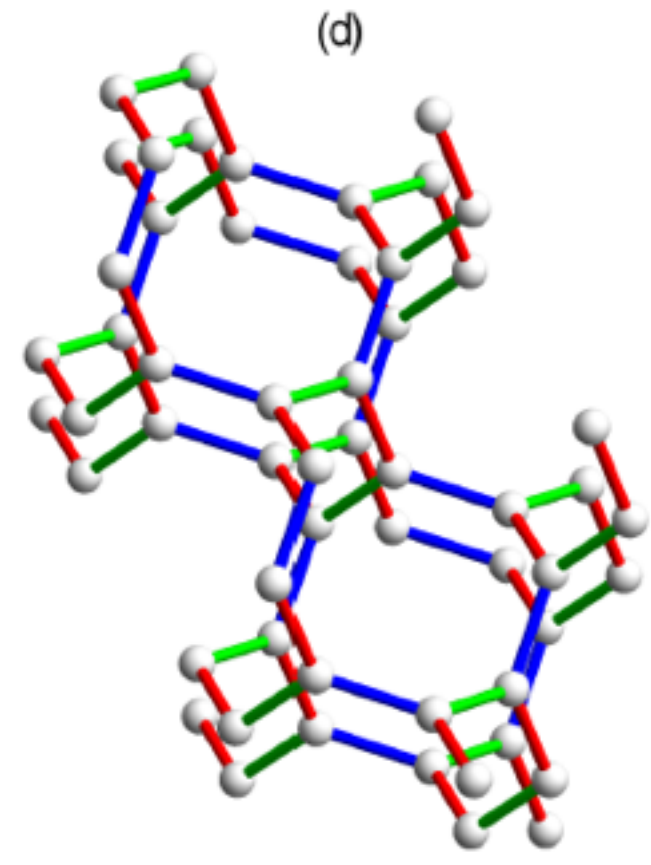
For each model, the low-energy(gapless) response is determined by the nodal structure of the fermions.



closed line of Dirac nodes

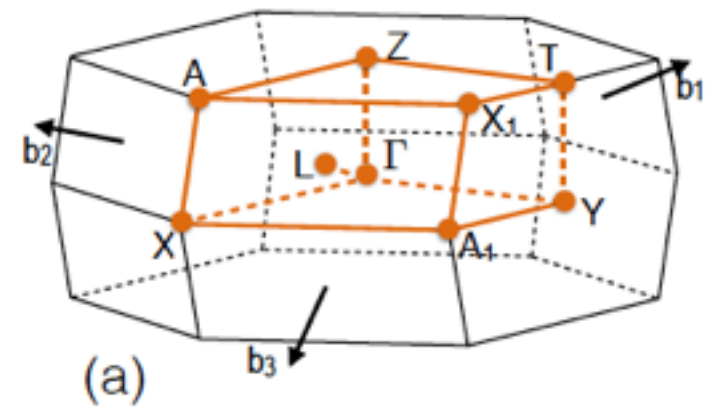
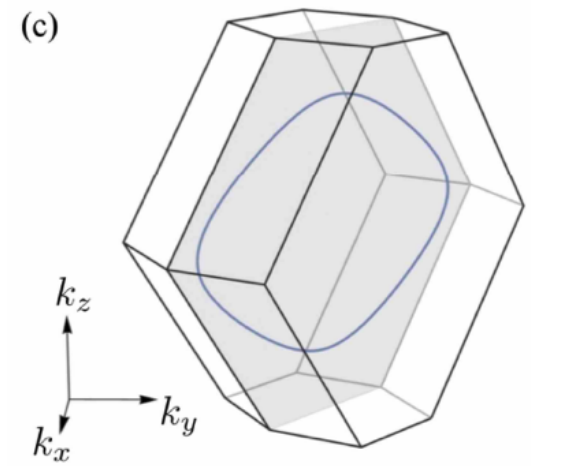
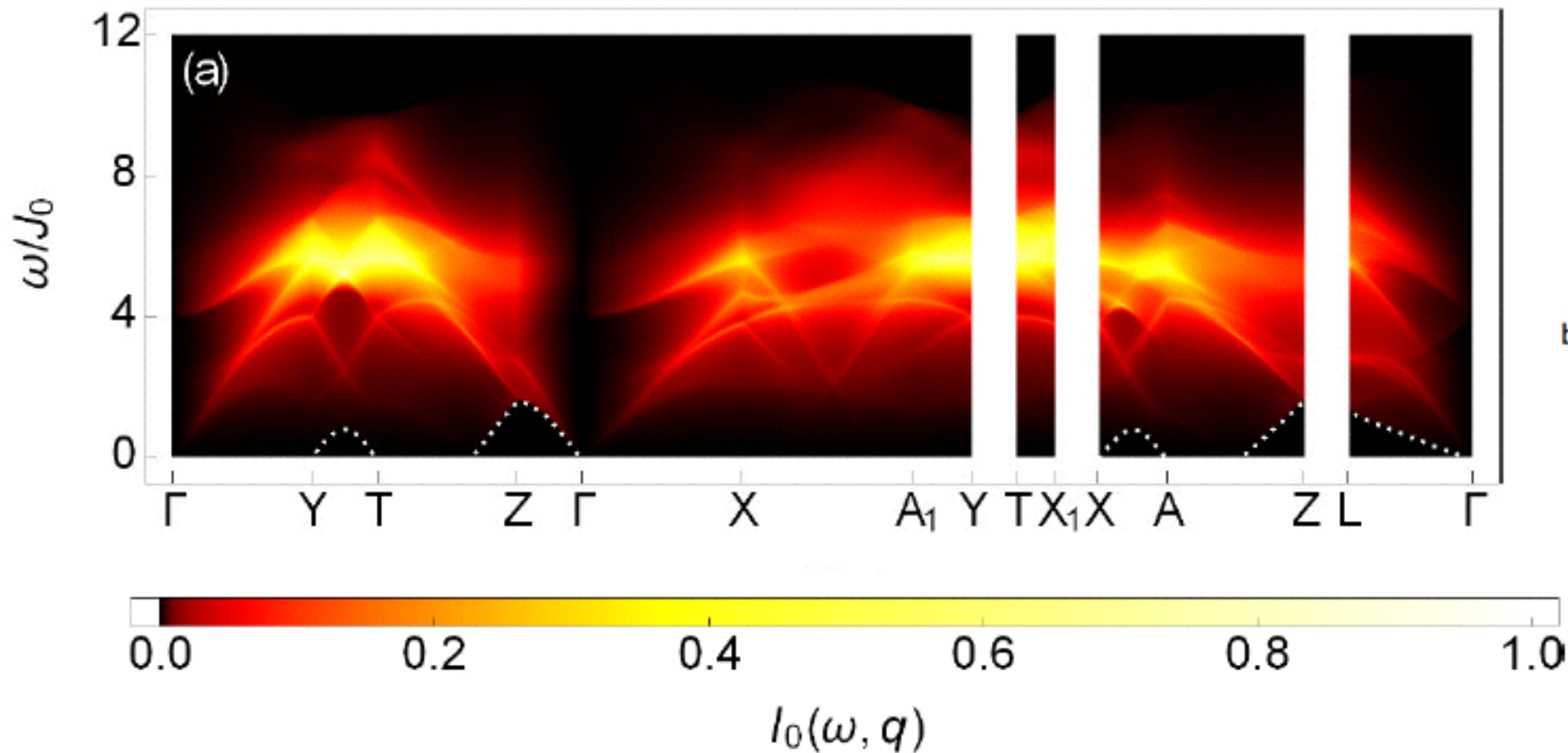


gapless Weyl points



Fermi surfaces

Hyperhoneycomb lattice

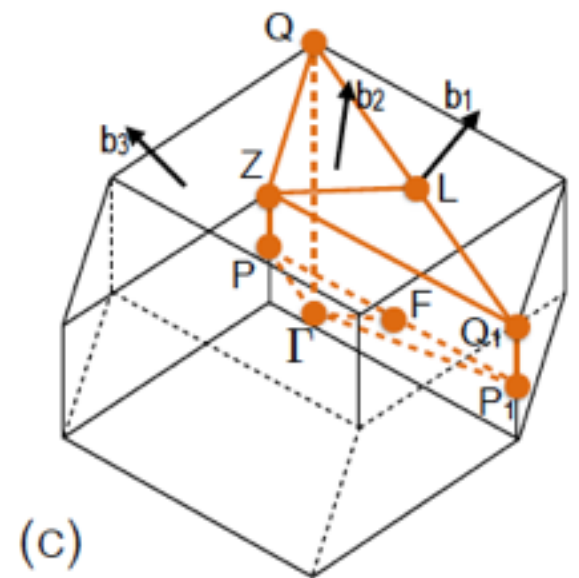
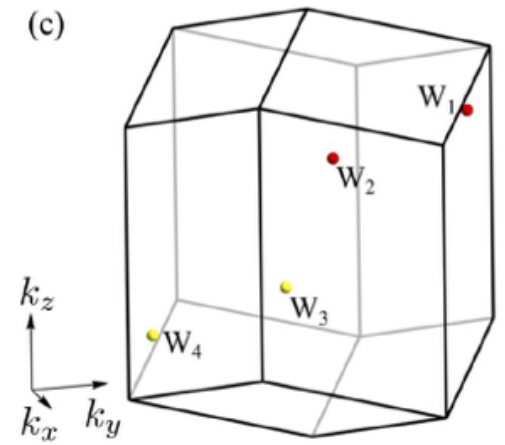
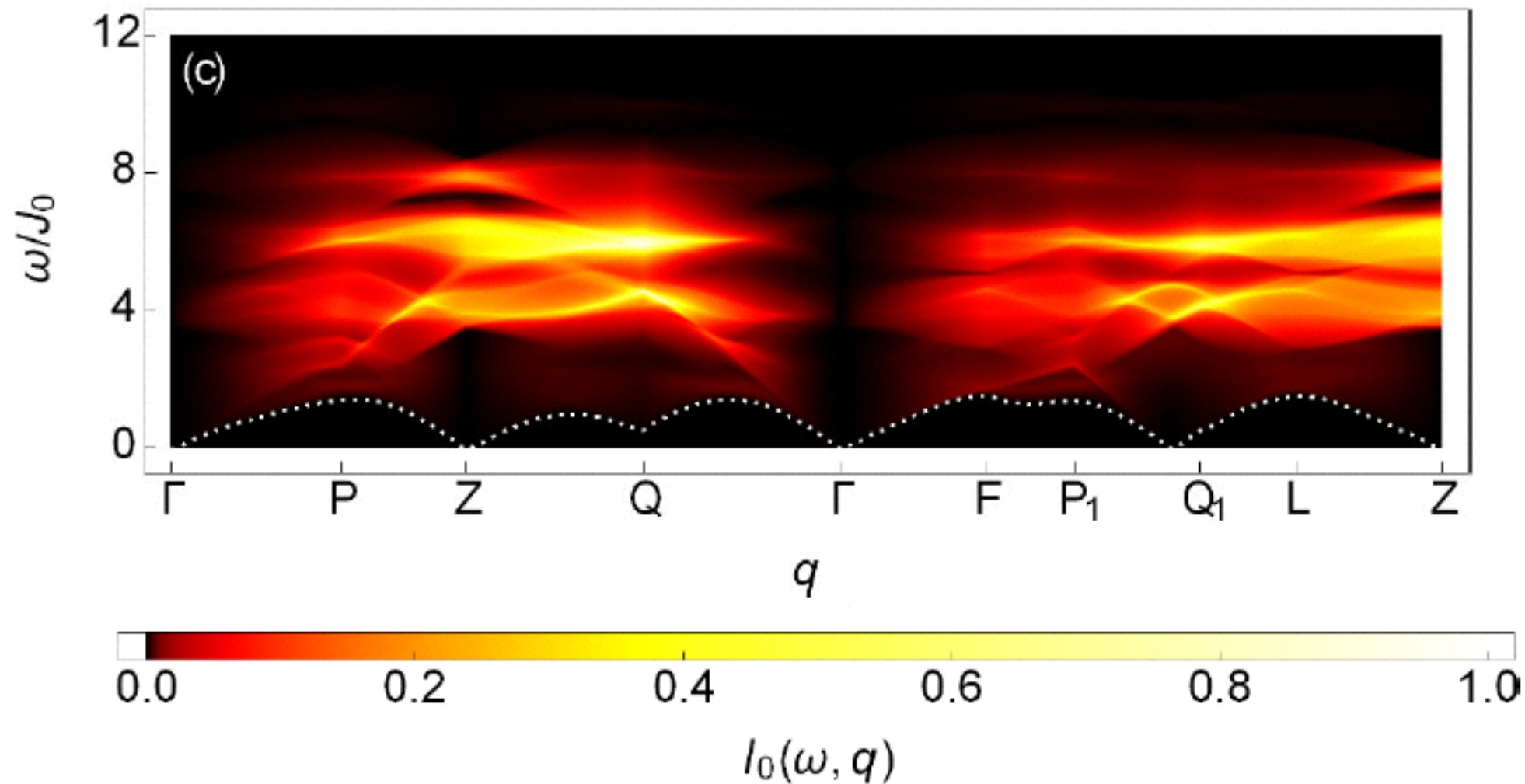


The Majorana fermions are gapless along a nodal line within the Γ -X-Y plane.



The response is thus gapless in most of the Γ -X-Y plane and also in most of the Z-A-T plane. However, it is still gapped at a generic point of the BZ.

Hyperhexagon lattice

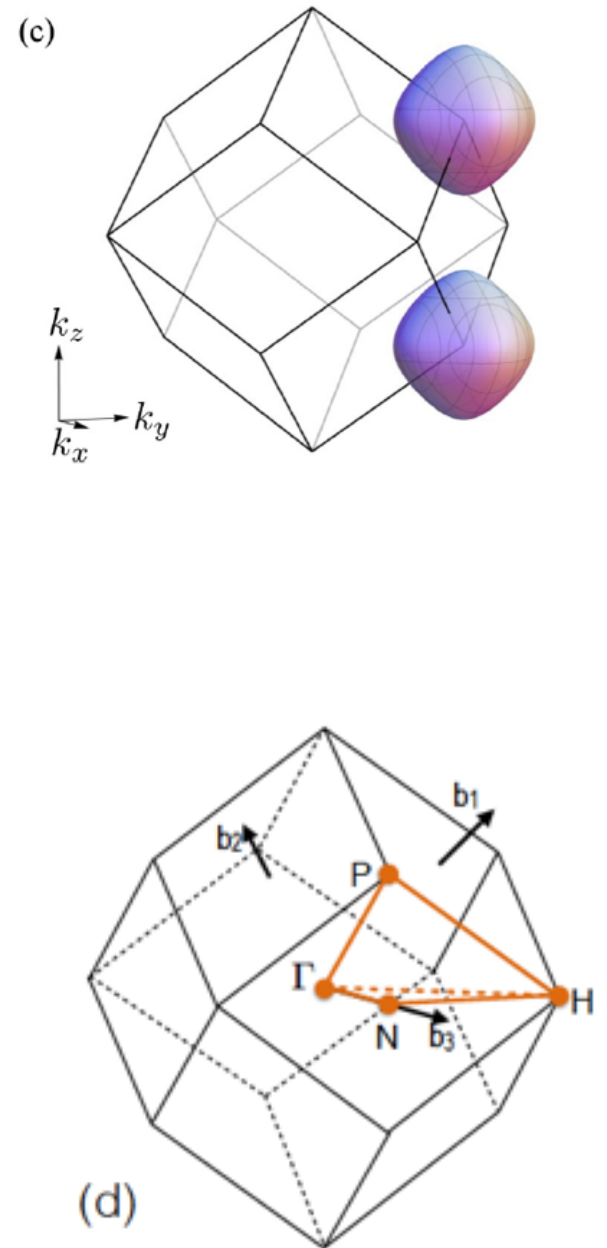
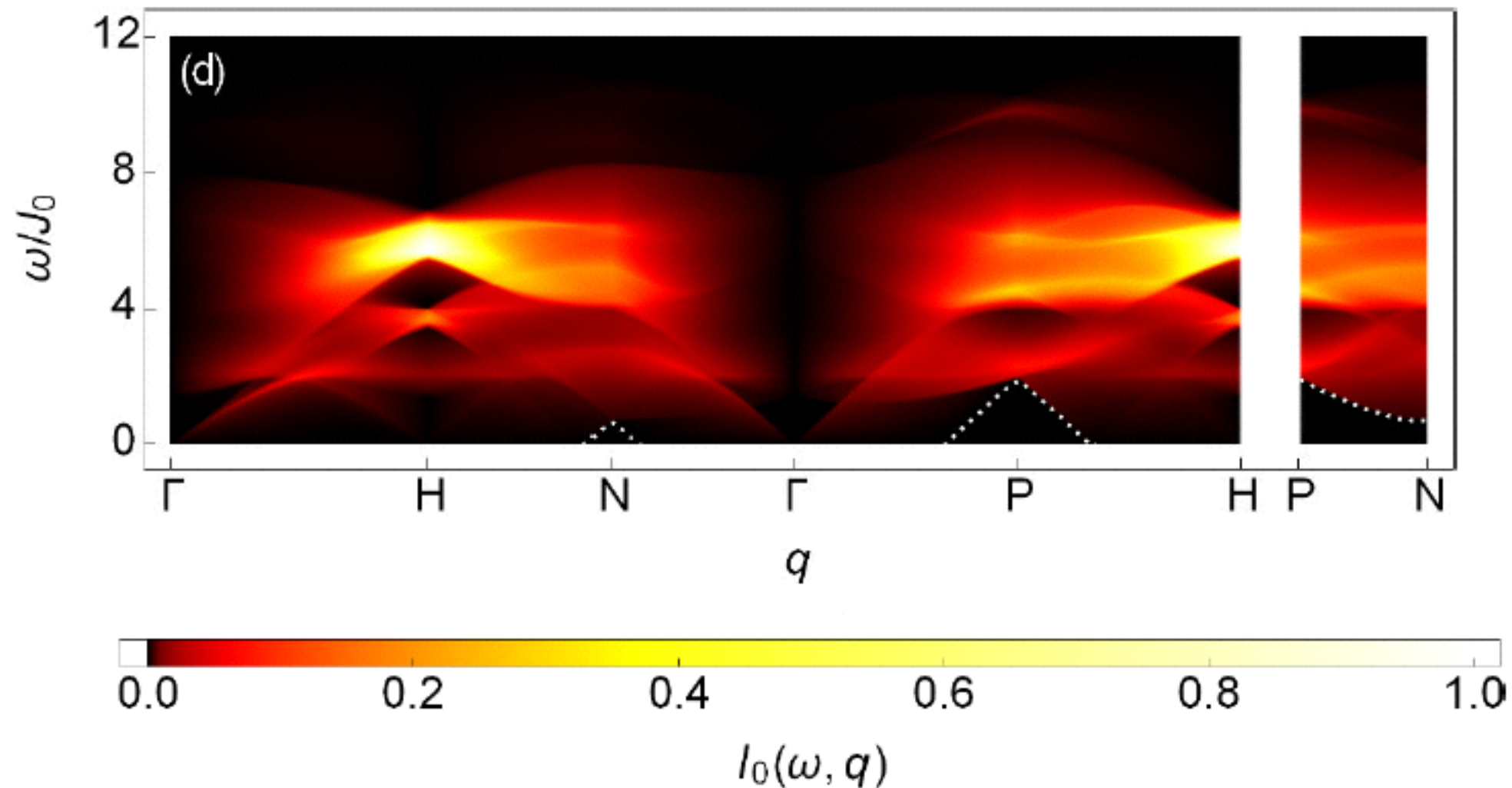


The fermions are gapless at Weyl points.



The response is thus only gapless at particular points of the BZ.

Hyperoctagon lattice



The Majorana fermions are gapless on a Fermi surface.



The response is thus gapless in most of the BZ.

Thank you